

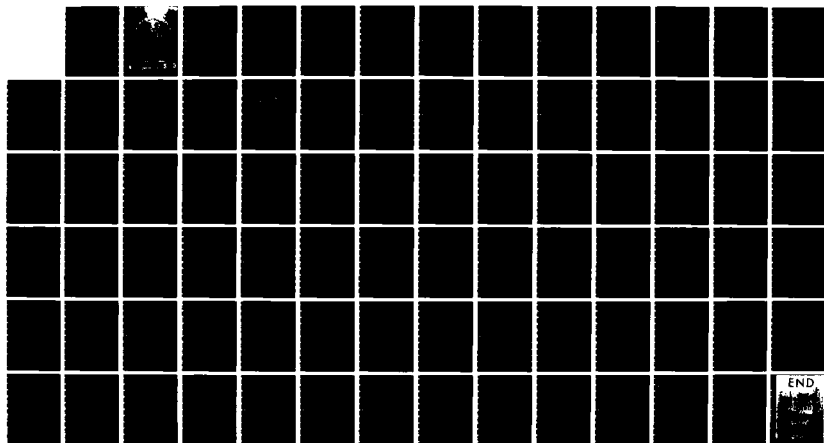
AD-A136 925

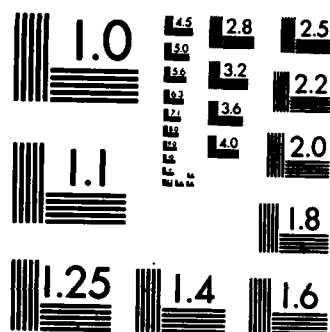
SUSTAINED LOAD CRACK GROWTH IN INCONEL 718 UNDER
NON-ISOTHERMAL CONDITIONS(U) AIR FORCE INST OF TECH
WRIGHT-PATTERSON AFB OH SCHOOL OF ENGI... D L MILLER
DEC 83 AFIT/GAE/AA/83D-15 F/G 20/11

1/1

UNCLASSIFIED

NL





MICROCOPY RESOLUTION TEST CHART
NATIONAL BUREAU OF STANDARDS-1963-A

AD A136925

AIR FORCE INSTITUTE OF TECHNOLOGY



AIR UNIVERSITY
UNITED STATES AIR FORCE

SUSTAINED LOAD CRACK GROWTH
IN INCONEL 718
UNDER NON-ISOTHERMAL CONDITIONS

THESIS

Douglas L. Miller
Captain, USAF

AFIT/GAE/AA/83D-15

DTIC FILE COPY

SCHOOL OF ENGINEERING

DTIC

ELECTE

JAN 17 1984

WRIGHT-PATTERSON AIR FORCE BASE, OH

This document has been approved
for publication and distribution
is unlimited.

84 01 17 075

AFIT/GAE/AA/83D-15

①

SUSTAINED LOAD CRACK GROWTH
IN INCONEL 718
UNDER NON-ISOTHERMAL CONDITIONS

THESIS

Douglas L. Miller
Captain, USAF

AFIT/GAE/AA/83D-15

DTIC
S
E

SUSTAINED LOAD CRACK GROWTH IN INCONEL 718
UNDER NON-ISOTHERMAL CONDITIONS

THESIS

Presented to the Faculty of the School of Engineering
of the Air Force Institute of Technology
Air University
In Partial Fulfillment of the
Requirements for the Degree of
Master of Science in Aeronautical Engineering



Douglas L. Miller, B.S., M.A.
Captain, USAF

December 1983

Accession For	
NTIS GRA&I	<input checked="checked" type="checkbox"/>
DTIC TAB	<input checked="checked" type="checkbox"/>
Unannounced	<input type="checkbox"/>
Justification	
By _____	
Distribution/	
And/or Codes	
11/or	
Dist. 11/1	
A-1	

Preface

The Retirement-for-Cause program will save the USAF valuable time and money. Crack growth in aircraft components often lead to catastrophic results. Being a pilot, I am well aware of these results. I have lost some close friends due to fatigue failure of aircraft components. I chose this investigation to add to my personal knowledge of the fatigue process and perhaps add a small piece to the puzzle of predicting crack propagation.

I have investigated crack growth under constant load and variable temperature because I had not found any published information in this region; yet, I considered it a main ingredient in understanding crack growth under thermal-mechanical loading.

I am very grateful to Mr. G. A. Hartman, UDRI, for setting up the microcomputer heating apparatus, and his constant help in testing and reducing data. I also thank Dr. T. Nicholas, AFWAL/MLLN, for his suggestions and help in analyzing some of the test results. The overall guidance of Major G. K. Haritos, AFIT/ENY, was critical and much appreciated throughout this investigation.

The patience and support of my family, especially my lovely wife, Allison, was very instrumental in my work and writing. To them I am indebted and am sincerely grateful.

Douglas L. Miller

Table of Contents

	Page
Preface	ii
List of Figures	iv
List of Tables	vi
Abstract	vii
I. Introduction	1
Background	1
Objective	3
Scope	4
Approach	4
II. Description of Test Apparatus	6
III. Test Procedures	13
IV. The Non-Isothermal Creep Crack Growth Rate Model	21
V. Experimental Results and Discussion	33
VI. Conclusions and Recommendations	49
Conclusions	49
Recommendations	51
Appendix A: Heat Treatment History of Test Specimens	52
Appendix B: "Crack Growth Rate Versus the Stress Intensity Factor" Curves	53
Appendix C: Tabulated Raw Test Data	57
Bibliography	69
Vita	70

List of Figures

Figure	Page
1. Heating Zones and Lamp Arrangement.	8
2. Test Specimen Geometry.	10
3. Programmed vs Temperature Response for an 8C/sec Triangular Wave Form.	11
4. Reduced Isothermal Baseline Data and Curve Fit. . . .	16
5. Isothermal Baselines Used to Predict Non- Isothermal Crack Growth Rates	17
6. Crack Growth Rate vs Temperature for the Isothermal Baselines.	22
7. Slope (n) of da/dt vs T Curves Plotted Versus K.	23
8. Linear Temperature Variation with Time.	24
9. Temperature Cycle with No Hold Time	26
10. Temperature Profile with Hold Time.	27
11. Non-symmetric Temperature Profile of the Proof Test.	28
12. Transition Crack Growth Rate Curve for Specimen Number 81-246 from 648C to 537C to 593C	35
13. Transition Crack Growth Rate Curve for Specimen Number 81-247 from 648C to 593C to 648C	36
14. Individual Type 1 Crack Growth Rates for Various Temperature Change Rates Compared to the Average of all Data	38
15. Type 1 Prediction Compared to the Average of all Type 1 Data	39
16. Test Data and Prediction for the Type 2 Test with a 3 Minute Hold Time.	41
17. Prediction and Data for the Type 3 Test with a 3 Minute Hold Time	42

Figure	Page
18. Prediction and Data for the Type 3 Test with a 15 Minute Hold Time	44
19. Crack Growth per Cycle for the Type 3 Tests	45
20. Prediction and Data for Both Type 4 Tests	47
21. Prediction and Data for the Proof Test.	48

List of Tables

Table	Page
I. Exact Specimen Dimensions and Total Precrack Length. .	12
II. Seven Types of Tests Conducted	15
III. Summary of Test Types and Parameters	20

Abstract

This investigation found linear cumulative damage modeling applicable to creep crack growth under non-isothermal conditions. The best results are obtained for high crack growth rates produced either by high temperature (above 593C), or by high stress intensities (K greater than 50 MPa \sqrt{m}). Except for one test, the linear model predicts conservative growth rates.

Constant temperature data are collected for 537, 593, and 648C and presented as da/dt vs K curves. Center-cracked specimens of Inconel 718 are used. The isothermal baseline data are used to predict crack growth rates for the non-isothermal tests using linear cumulative modeling. Specimens are subjected to low frequency thermal cycling between 537C and 648C. Constant load is always maintained throughout each test. Temperature is changed in the vicinity of the crack by using four infrared quartz halogen lamps. This allows realistic temperature changes in short periods of time, approximately 4.6C/second. A micro-computer maintains the desired temperature profile. Various hold times and temperature change rates are used.

The predicted creep crack growth rates were within a factor of two of the actual test data. The time-to-failure, predicted for one test, is 56 percent of the actual time to failure.

SUSTAINED LOAD CRACK GROWTH IN INCONEL 718 UNDER NON-ISOTHERMAL CONDITIONS

I Introduction

Background

The current USAF policy for removing aircraft engine components from service, when they have reached their low cycle fatigue design lifetime, has proven to be extremely conservative. It is based on the prediction that 1 in 1000 engine disks will develop a 0.03 in. crack in one design lifetime (1). This forced retirement policy requires the elimination of 999 statistically sound disks in order to remove the one cracked disk. In addition, even this cracked disk may have some useful crack propagation life remaining. Although this forced retirement policy is extremely conservative, it is also deemed necessary for critical components, owing to the lack of appropriate guidelines on safe fatigue crack growth limits. The USAF is pursuing a research program called "Retirement-for-Cause" (RFC). Its objective is to use each component based upon a statistically safe design life, RFC requires inspection of the components at designated intervals and retirement of components only after an unsafe crack has been discovered.

Two requirements are essential to safely utilize this RFC program. The first is a reliable nondestructive examination procedure to detect cracks which are larger than the predetermined rejection size. The second requirement is to accurately predict the crack growth rate under mission conditions. This requirement includes determining accurate stress and temperature fields of the components subjected to the mission

conditions. This research project addresses the last requirement, predicting crack propagation rates.

The effects of temperature cycling on the creep rate of materials have been studied since the early 1950's. E. L. Robinson (2) developed theoretical formulas for predicting the rupture life under cyclic temperature based upon constant temperature data. He assumed that the life expended in any portion of the temperature cycle is independent of the rest of the cycle. He does not account for transition or retardation effects. J. Miller (3) performed experiments to verify Robinson's theory. Using Robinson's formulas, he predicted the life to rupture of various high temperature alloys. Most of his test results fall between the calculated value and one half of the calculated value. He, too, ignored transition effects.

Carreker, Leschen, and Lubahn (4) suggested that some transient effects may contribute to the creep rate when the temperature is changed. They observed extensive retardation in the creep rate for copper and lead wires after lowering the temperature. All of these works were concerned with creep rates in uncracked specimens.

Linear elastic fracture mechanics (LEFM) has been used successfully to predict the fatigue lifetime of components under low temperature isothermal conditions. More recently, LEFM has been extended to the higher temperature range where there may be some localized nonlinear deformation occurring (5). Very little crack propagation data has been obtained for cyclic thermal loading under constant mechanical loading, or for combined cyclic stress and thermal loading. C. A. Rau, et al (5), demonstrated that LEFM may be applied to thermal-mechanical

fatigue crack propagation of nickel-and cobalt-base superalloys under small plastic strain conditions. They also compared isothermal growth rates to thermal fatigue growth rates. They determined that at lower temperatures (426-760C), the cyclic thermal loading generally produces a higher growth rate than isothermal conditions. They attribute this to effective crack resharping.

Shahinian and Sadananda (6) examined crack growth behavior in Alloy 718 plate under cyclic and static loads at elevated temperatures over a wide range of conditions. They tested the applicability of the fracture mechanics method to crack growth under conditions well into the creep range. The inverse of the usual temperature dependence of crack growth rate holds true for Inconel 718 at temperatures above 648C (6). Here, creep effects seem to retard crack growth especially as the hold times increase. When this occurs, LEFM must be used with caution (6). Generally, their test failures occurred earlier than predicted by the linear damage rule.

General Electric Company (7) has investigated the hold time and thermal mechanical effects on the fatigue life of various alloys. Studies currently in progress examine the behavior of Inconel 718 under combined stress and thermal cycling. There apparently is no data available concerning creep crack growth under cyclic thermal conditions.

Objective

This investigation addresses creep crack growth under non-isothermal conditions and investigates the applicability of linear cumulative damage modeling. This is done by obtaining isothermal baseline data and integrating their contribution to a series of non-isothermal crack

growth experiments. Results are analyzed to determine the applicability of linear cumulative damage modeling. The impact of ignoring transient effects, resulting from temperature changes, is examined.

Scope

Non-isothermal creep crack growth testing was conducted using centercracked specimens of Inconel 718. Specimens were subjected to low frequency thermal cycling under sustained loading. Temperature cycled between 537 and 648C (1000 and 1200F) using a trapezoidal wave form. Hold times at the high and low temperature settings varied from 0 to 15 minutes. Longer hold times were used to examine transient effects after the temperature changed. Three temperature change rates were used: 4.625C/sec, 1.68C/sec, and 0.4625C/sec. The data thus collected, were compared to the isothermal baseline data. A simple model for the predictions of the crack growth rate is proposed. The predicted results for the various tests are plotted and compared to the experimental results. In addition, non-symmetric wave shapes and simple temperature spectra were considered to examine the applicability of the proposed prediction model to more complex temperature conditions.

Approach

Isothermal baseline data were collected and reduced, and are presented as da/dt versus K curves, where a is crack length, t is time, and K is the stress intensity factor at the crack tip. One curve was made for each of three temperatures: 537, 593, 648C. From these baseline curves, da/dt versus temperature plots are made for individual K values. This produces da/dt as a function of temperature.

Temperature changes were applied as a series of continuous cycles. The temperature was controlled and varied with time; therefore, da/dt can be expressed as a function of time. From this expression, the crack growth rate for specific temperature profiles was predicted. Tests were conducted in which the rate of temperature change, hold times, and sudden excursions from high to low and low to high temperatures were varied, one at a time. These test results were plotted and compared to the baseline data and to the predictions. Finally, a predicted growth rate was computed for a proof test in which non-symmetric rates and hold times were used. The proof test results were compared to this prediction to investigate the applicability of the procedure to more complex conditions. Using the predicted growth rate, the time-to-failure for the proof test was calculated. This predicted failure time was compared to the actual time to failure.

II. Description of Test Apparatus

The thermal-mechanical test apparatus consists of six major components. These are:

1. A microcomputer used as a controlling unit
2. A furnace frame with 4 power controllers and 4 quartz lamp heaters
3. A coolant controller and two coolant jets
4. An Arcweld creep frame
5. A test specimen
6. A traveling microscope used to measure crack length.

The microcomputer is a Research Incorporated Micricon Model 82300 with four closed loop controller channels for K-type thermocouples. This unit provides pre-programmed independent control of the four heating lamps. It also turns the cooling system on and off at the appropriate times. The ability to independently control the four heaters is essential in order to maintain a constant temperature profile near the crack tip. This microcomputer also has the capability to program different mechanical loading and temperature profiles and maintain a preferred phase relationship between them.

The microcomputer controls temperature as a function of time. The system is capable of heating and cooling a specimen at a rate of 8C/sec. This rate is accomplished under closed loop control. Actual temperature profiles of a trapezoidal wave form are found to be within 10C of the program. This system maintains constant temperature over the specimen width to within 5C. A maximum heating rate of 20C/sec may be achieved,

but at that rate the temperatures within the heating zones vary $\pm 35^{\circ}\text{C}$ from the desired profile (8).

The furnace frame is attached to the mechanical loading machine and contains the microscope, four power controllers and quartz lamps, and two coolant jets. Test specimens may be replaced without disturbing the frame. Each controller adjusts the power supplied to its corresponding 1000-watt quartz lamp. Each heating zone temperature, shown in Fig 1, is independently controlled. The lamps are arranged to produce four overlapping heating zones (2 in. X 1.5 in. each) and yet allow full view of the crack throughout the test. The high intensity light produced by the quartz lamps aids in crack tip measurements. Five thermocouples are spotwelded to the specimen as shown in Fig 1. The one closest to the center of the crack is not incorporated in the temperature controlling process; it only provides temperature data.

The cooling system uses an on/off solenoid to control the flow of compressed air, at room temperature, to the jets. The jet arrangement is shown in Fig 1. Two 0.25 in. diameter copper tubes with 0.050 in. outlet holes provide an updraft of cooling air on the back side and a downdraft of air on the front side of the specimen. An overflow of cooling air is used so that additional heating is required. By overcooling and compensating with the more accurate controlled heaters, the desired cooling rate is achieved. For most tests, the time required to heat the specimen to the maximum temperature (648°C , 1200°F) from the minimum temperature (537°C , 1000°F) is 24 seconds. At this rate, the temperature stays with $\pm 3^{\circ}\text{C}$ of the desired profile, producing a rate of $4.625^{\circ}\text{C}/\text{sec}$. This rate was chosen as the primary rate to gain more

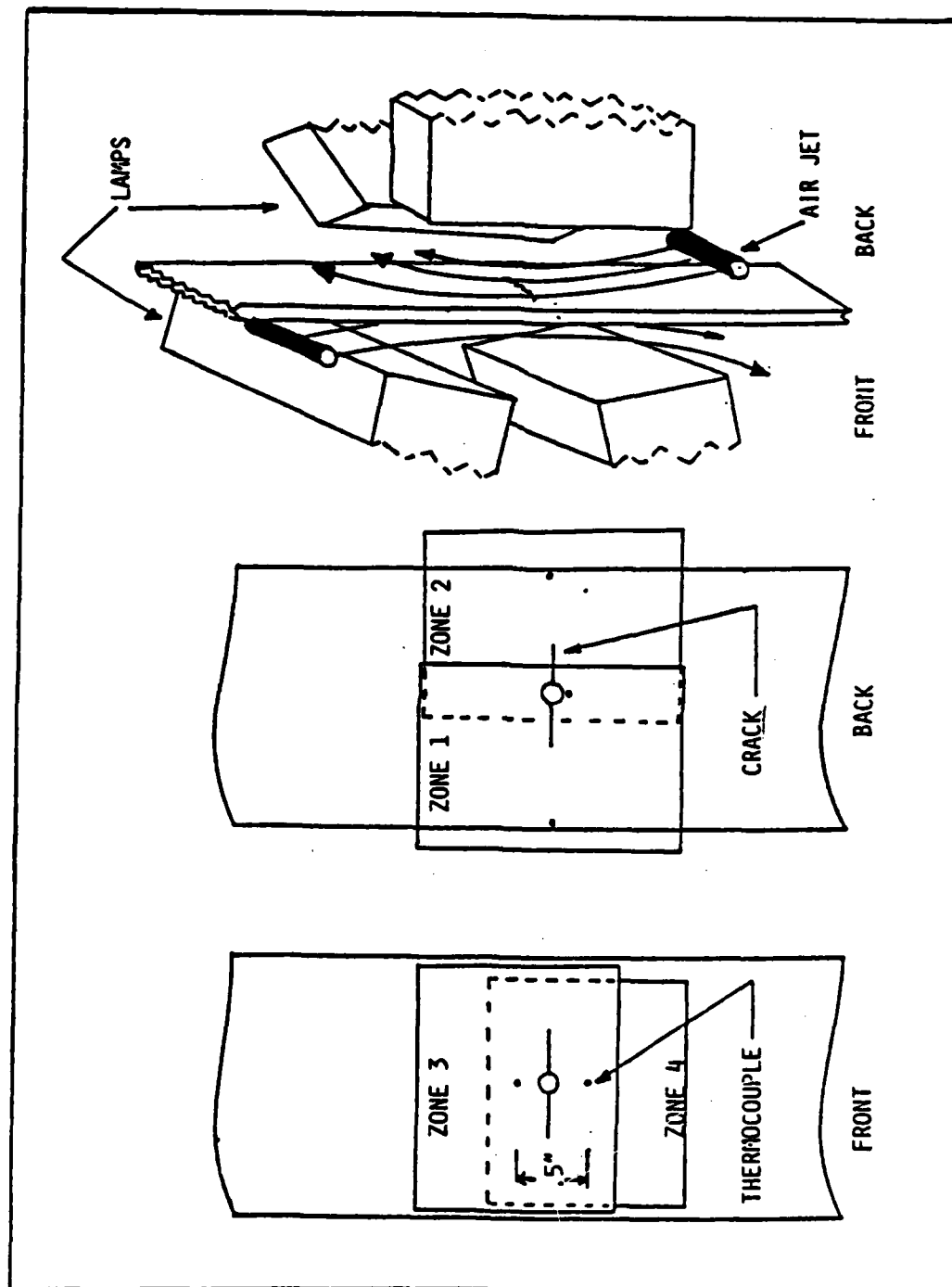


Figure 1. Heating Zones and Lamp Arrangement

temperature control and better simulate mission profiles.

An Arcweld lever arm creep frame with a 1200-pound capacity (dead weight) is the loading apparatus.

The test specimens are standard center-cracked specimens of Inconel 718, approximately 2.000 in. wide and 0.095 in. thick. Exact specifications are listed in Table I. The specimens were heat-treated as shown in Appendix A. The flat plate specimen was chosen because of its high surface area to volume ratio, resulting in the fastest heating/cooling rates with the least amount of through-the-thickness temperature variation. The maximum through-the-thickness temperature variation measured on a test specimen was 4C. Figure 2 shows the typical specimen geometry and dimensions.

A Gaertner 10X traveling microscope is used to measure crack length. The effective crack length resolution is approximately 0.001 in., when aided by the high intensity light of the quartz lamps.

Figure 3 plots the response of this system to a temperature change rate of 8C/sec in a triangular wave form. The lag time is one second or less and the variance is no more than ¼C. This newly developed system offers excellent control over rapid temperature changes for any number of cycles. It also has the potential capability of simultaneously controlling mechanical and thermal loading, and the phasing between them.

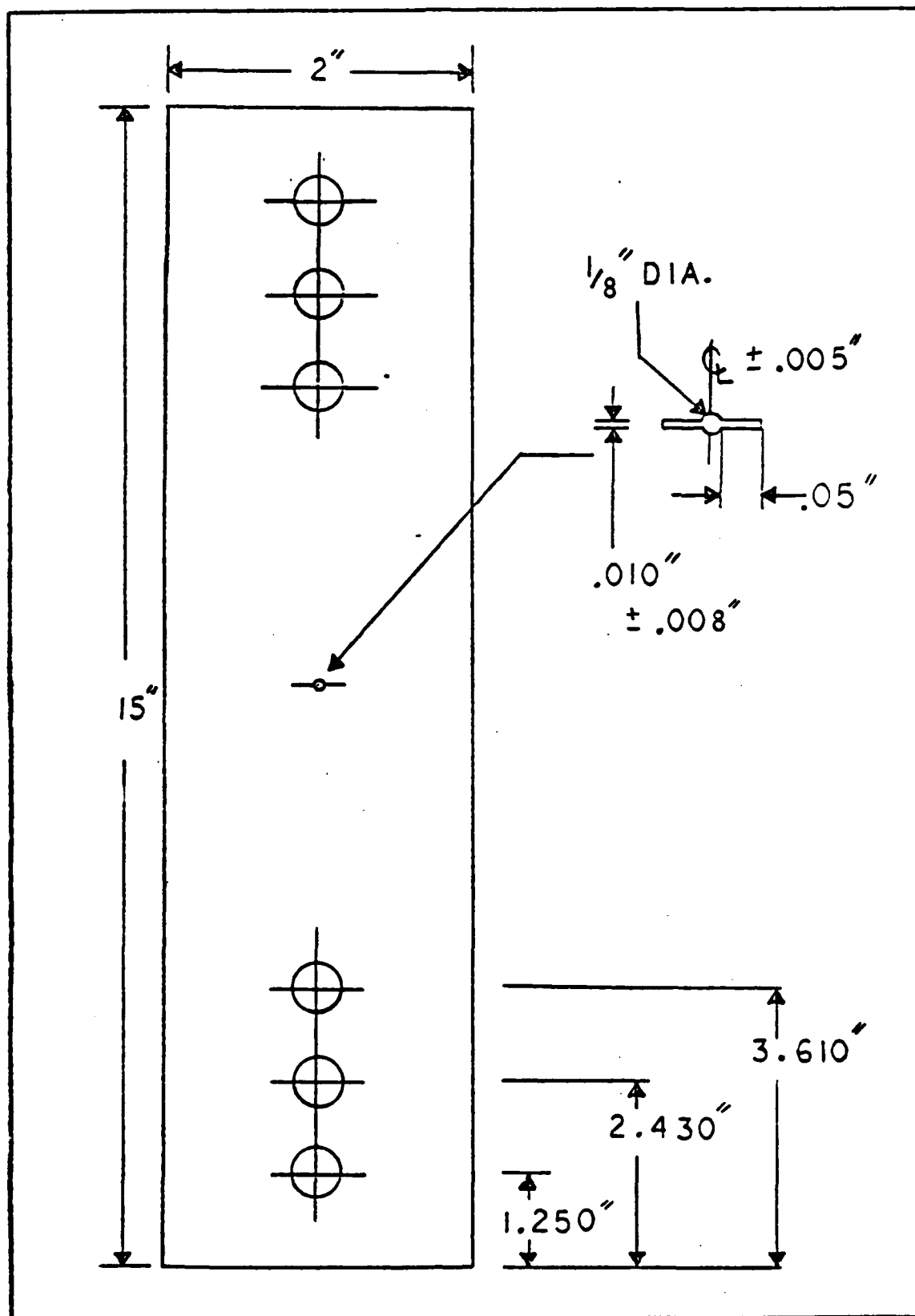


Figure 2. Test Specimen Geometry

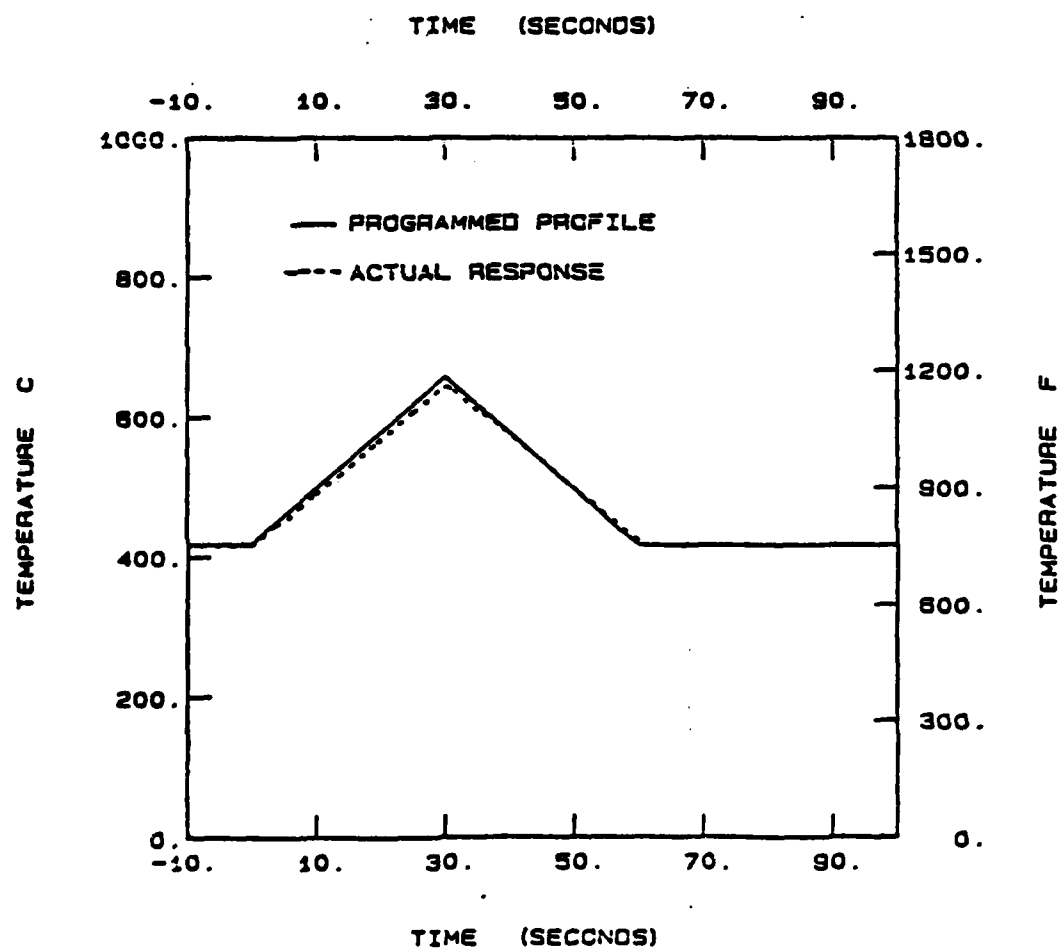


Figure 3. Programmed vs Temperature Response for an 8C/sec Triangular Wave Form.

Table I

Exact Specimen Dimensions and Total Precrack Length
All measurements are in inches.

SPECIMEN NO.	WIDTH	THICKNESS	PRECRACK 2a
81-212	1.988	0.097	0.252
81-214	1.987	0.094	0.428
81-216	1.985	0.093	0.458
81-217	1.962	0.095	0.288
81-217W	1.962	0.095	0.354
81-218	1.989	0.095	0.350
81-227	1.989	0.093	0.400
81-231	1.988	0.096	0.282
81-239	1.965	0.095	0.296
81-240	1.987	0.095	0.302
81-240W	1.987	0.095	0.378
81-241W	1.986	0.093	0.290
81-242	1.987	0.096	0.278
81-244	1.987	0.096	0.348
81-244W	1.987	0.096	0.324
81-246	1.990	0.096	0.328
81-246W	1.990	0.096	0.316
81-247	1.990	0.096	0.324
81-250	1.988	0.096	0.320
81-252	1.989	0.096	0.372
81-254	1.989	0.096	0.308

III. Test Procedures

The IN 718 specimens are drilled with grip holes. A through-the-thickness starter crack, approximately 0.225 inches long, is electric-discharge machined (EDM) in the center of the specimen (see Fig 2 for test specimen dimensions and geometry). The specimen is then precracked, at room temperature, on an MTS servohydraulic test machine, to approximately 0.25 to 0.30 inches total crack length using a 10 Hz sine wave form. The local stress intensity factor near the crack tip (K) during precracking is below 20 ksi (in)^{1/2}. The crack length, after precracking, for each specimen is given in Table I.

During overnight test shutdowns, the load was removed, but the lamps were allowed to cycle to maintain the desired temperature profile. For longer downtimes, both temperature and load were removed. These shutdown times are indicated on the da/dt vs K curves by arrows placed either above or below the curve. Shutdown times seem to have a temporary retardation effect on the crack growth. These effects are ignored during curve smoothing procedures.

The raw data for each test are given in Appendix C. The data for crack length as a function of time were reduced using a seven point sliding polynomial routine. The reduced data were plotted as da/dt vs K curves. To alleviate the problem of local crack tip delays and accelerations, the reduced data plot was fitted using the "french curve" approach. This approach manually fits the data to the best visual fit using a french curve. This has been shown to be the easiest and least controversial method to curve fit (3). Figure 4 shows the reduced

baseline data with the "french curve" fit for all three individual temperatures. Seven types of tests (shown in Table II) were conducted.

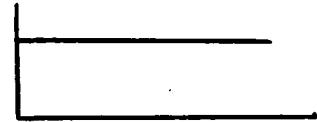
Baseline data were collected under isothermal, constant load conditions. Tests were conducted at 648C (1200F), 593C (1100F), and 537C (1000F). The constant load was generally different for each test; however, some groups of tests were accomplished under the same load. This was done for both comparison and convenience. The "french curve" fits of the baseline data (Fig 4) were used to predict the results of the other types of tests. The isothermal baselines are shown without the data in Fig 5.

Transition time tests were conducted to determine the amount of time required for the crack growth rate to return to its normal baseline rate after the temperature was reduced from 648C to 593C or 537C. Temperature was changed at the rate of 4.625C/sec. The approximate magnitude of retardation of the growth rate can be seen from the transition tests' results. It was determined that the best technique for collecting transition test data at 648C, where there was rapid crack growth, was to record the crack length at 1.5 minute intervals for 30 minutes. During low temperature testing, measurements were taken at approximately 0.01 in. of total crack growth until 0.2 or more inches of growth had occurred. This technique accomplished two objectives. The first was to collect at least 15-20 data points at each temperature in order to obtain acceptable results from the seven point polynomial reduction routine. The second objective was to allow the crack to grow through the large plastic zone created by the 648C temperature and stabilize at the lower temperature baseline. Generally, 0.2 inches of

Table II

Seven Types of Tests

a. Isothermal Baseline



b. Transition Time



c. Type 1: No Hold Times



d. Type 2: Hold Time at Maximum Temperature



e. Type 3: Hold Time at Minimum Temperature



f. Type 4: Hold Time at Maximum and Minimum Temperature



g. Proof Test: Non-symmetric Hold Times and Rates



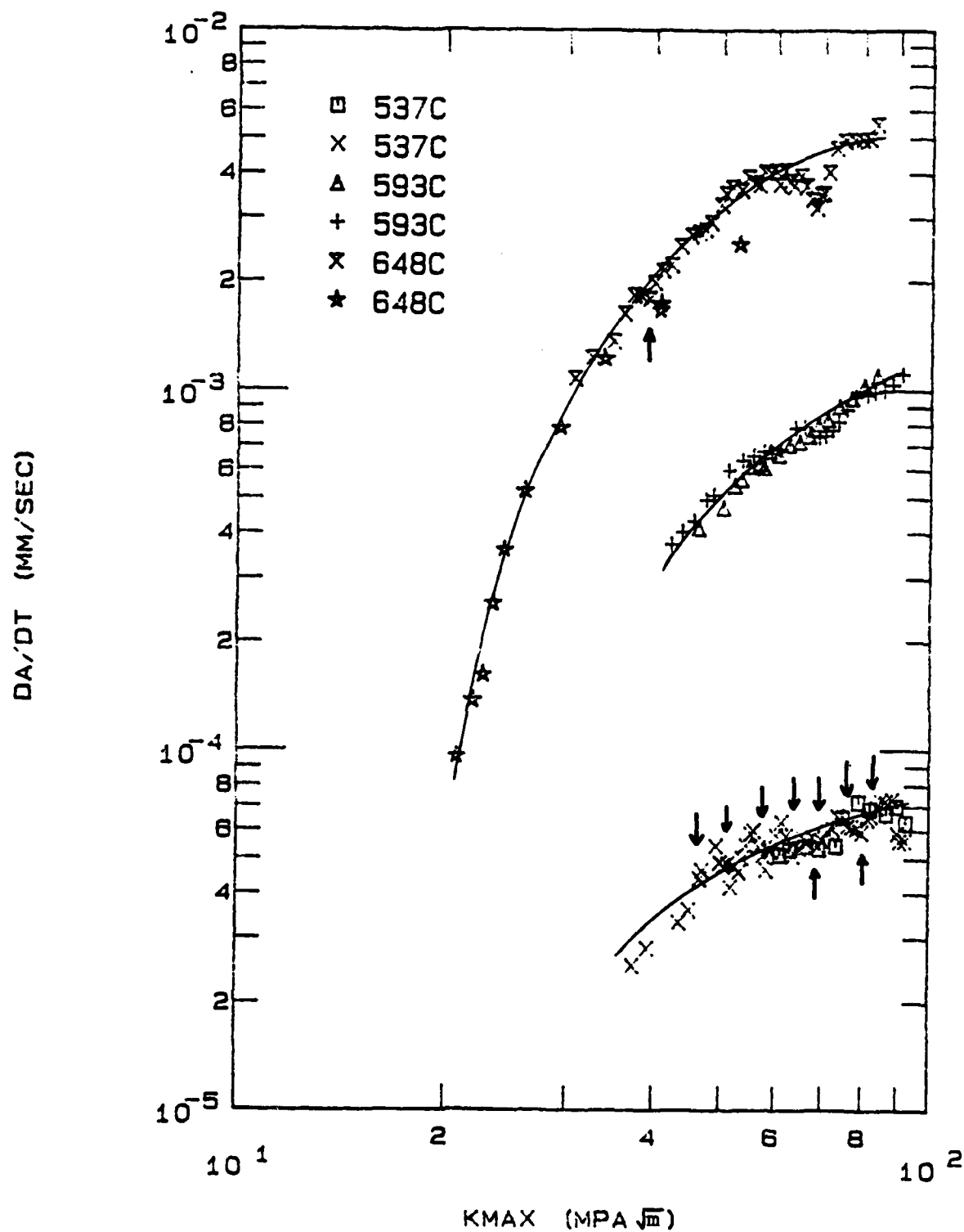


Figure 4. Reduced Isothermal Baseline Data and Curve Fit (solid lines)

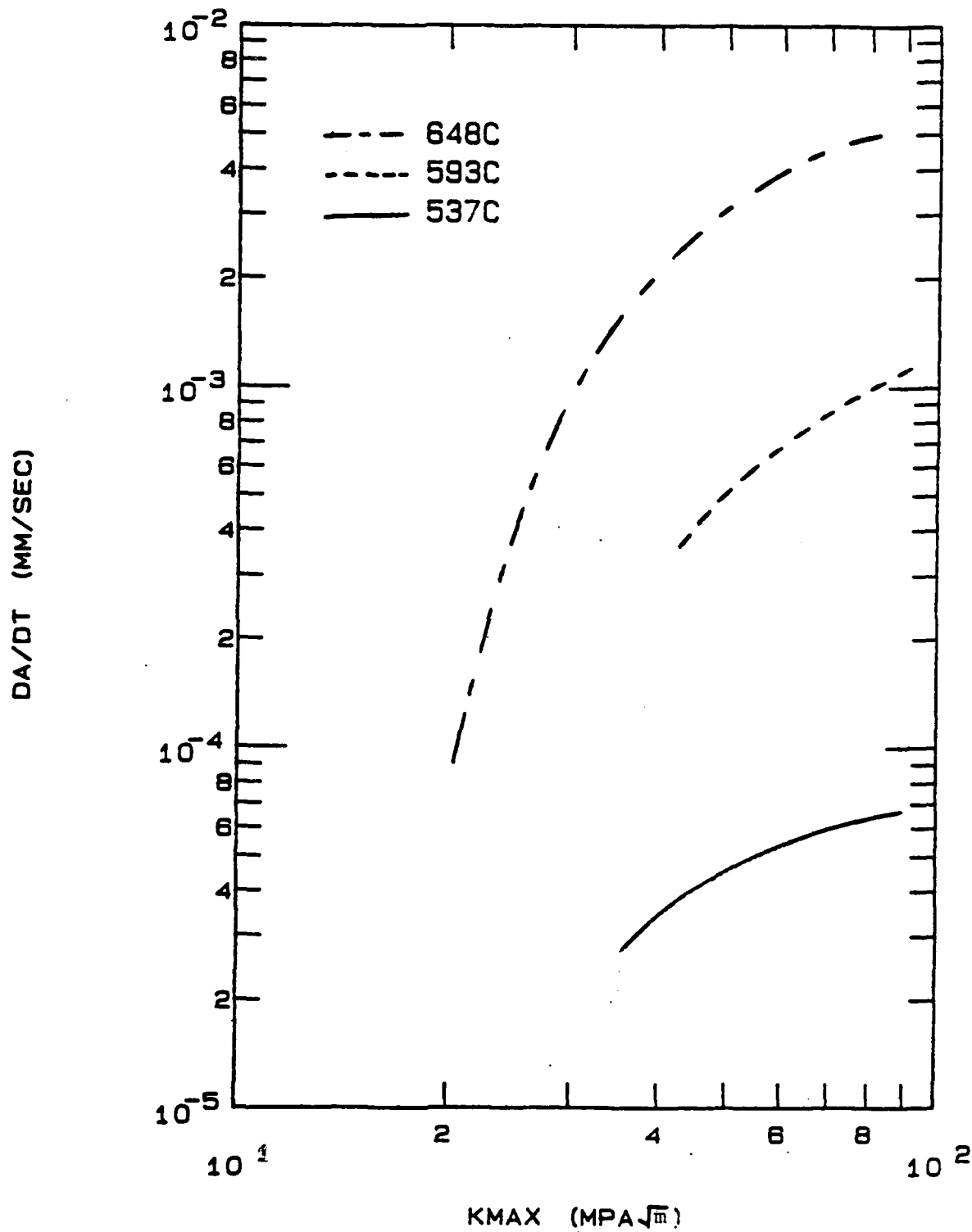


Figure 5. Isothermal Baselines Used to Predict Non-Isothermal Crack Growth Rates

total growth proved sufficient for meeting these objectives. To prevent the seven point reduction routine from averaging all data points during the transition tests, the routine was started for one temperature, completed, and then restarted for the next temperature.

All of the temperature cycling was achieved by programming the desired temperature profile into the microcomputer. The normal profile consisted of raising the temperature from room temperature to 648C in three minutes. This temperature was maintained for two minutes for final lamp adjustments. Using the selected rate, the temperature was lowered to either 593C or 537C. It was held there for the given hold time and raised again to 648C at the same rate and held there for the specified period of time. Throughout the test, the loads were held constant. Hold times varied from 0 to 15 minutes, well below the transition time which was determined to be approximately 60 minutes from the transition tests. Three different temperature change rates were used. The primary rate of 4.625C/sec gives a 24 second cycle for the 648/593C tests and a 48 second cycle for the 648/537C tests. This compares favorably with temperature changes obtained by turbine disks during takeoff of modern fighter aircraft (9).

During two Type 1 tests (see Table II), a rate of 1.68C/sec was used to determine what effects, if any, the rate of temperature change would have on crack propagation. This is also the same rate used by a previous study in which both temperature and load were cycled (7). Therefore, the results of constant load and cycle temperature tests could be compared to the results of combined cyclic load and temperature tests. A much slower rate of 0.4625C/sec was used in two tests

to further examine the effects of changing the rate. During the cyclic tests, crack measurements were taken during the period of temperature increase to take advantage of the improved illumination of the crack.

Types 2 and 3 (Table II contains example profiles) tests consisted of maintaining a constant base temperature and rapidly increasing or decreasing to the second temperature, with zero hold time, and returning to the base temperature. A rate of temperature change of 4.625C/sec was used. The hold times used at the base temperature were three and fifteen minutes.

The Type 4 tests incorporated the same hold time at both the high and low temperature. Three and fifteen minute hold times were used at a temperature change rate of 4.625C/sec.

The proof test involved a complex temperature profile (refer to Table II for a graphical representation). The increase rate was 3.03C/sec. The temperature was held at 648C for 60 seconds and then returned to 537C at a rate of 8.33C/sec. The hold time at 537C was 180 seconds.

Certain specimens were used to accomplish two separate tests. The first test was conducted to a predetermined K level and terminated. The second test was then started and continued to specimen failure. The first several data points collected during the second test were discarded to eliminate any effects of the first test.

The results plotted for each test are compared to baseline data and the predicted growth curve. The prediction is based upon linear cumulative damage modeling as explained in Chapter IV. All test conditions are summarized in Table III.

Table III

Summary of Test Types and Parameters

SPECIMEN NUMBER	TEST TYPE	TEMPERATURE (deg C)	LOAD (lbs)	K (MPa(m) ^{1/2})	
				START	END
81-212	Baseline	537	10873	43.27	100.2
81-244	Baseline	537	8023	34.88	116.3
81-250	Baseline	593	9390	40.32	98.0
81-239	Baseline	593	9390	37.84	101.5
81-231	Baseline	648	6408	24.62	93.0
81-242	Baseline	648	5126	20.07	71.6
81-217	48 sec cyc	648/537	6400	26.46	83.1
81-244W	48 sec cyc	648/537	6800	28.59	43.0
81-227B	132 sec cyc	648/537	5600	38.41	77.3
81-240	132 sec cyc	648/537	6400	25.59	77.2
81-218	480 sec cyc	648/537	6400	28.00	77.9
81-241WB	480 sec cyc	648/537	6000	44.04	80.0
81-246	Transition	648/537/593	7740	45.55	104.0
81-247	Transition	648/593/648	6400	26.95	81.6
81-252	Transition	593/648/593	7740	35.56	83.4
81-214A	Type 3	3 min hold @ 537	8800	43.43	92.5
81-216	Type 2	3 min hold @ 648	6400	32.64	85.0
81-246W	Type 3	15 min hold @ 537	10400	43.20	96.4
81-227A	Type 4	3 min @ 537/648	5600	26.24	39.0
81-217WA	Type 4	15 min @ 537/648	6400	28.21	44.3
81-240W	Proof	648/537	7600	34.72	96.7

IV The Non-isothermal Creep Crack Growth Rate Model

This section develops the models for predicting the crack growth rates for the various tests conducted in this experimental investigation. The rates of temperature change, or the hold time periods, or both, were varied between the different types of tests. Using the models developed in this section, the crack growth rates can be predicted, at a given stress intensity factor (K), for the non-isothermal tests conducted. The procedure for obtaining a predicted crack growth rate versus stress intensity factor plot (da/dt vs K) is outlined. The predictions are based on the crack growth rates and other information obtained solely from the isothermal baseline curves. No attempt is made to account for transient effects which occur during temperature changes. All predictions are made using linear damage modeling. An expression for predicting the time-to-failure, based upon the predicted crack growth rate curve, is also developed in this section. It should be noted here that any difference between the experimental crack growth rate and the predicted rate will affect the time-to-failure prediction.

The isothermal baseline results are shown in Fig 5; the crack growth rate (da/dt) is plotted versus the stress intensity factor (K). For a given K value, three different crack growth rates are available from this figure, each corresponding to a different temperature. From the data of Fig 5, Figure 6 is constructed; there the crack growth rate is plotted versus temperature on a logarithmic scale. Each curve represents a constant K value. For clarity, only the curves for the two extreme cases ($K=40$, $K=90$) are shown. It is assumed that these data

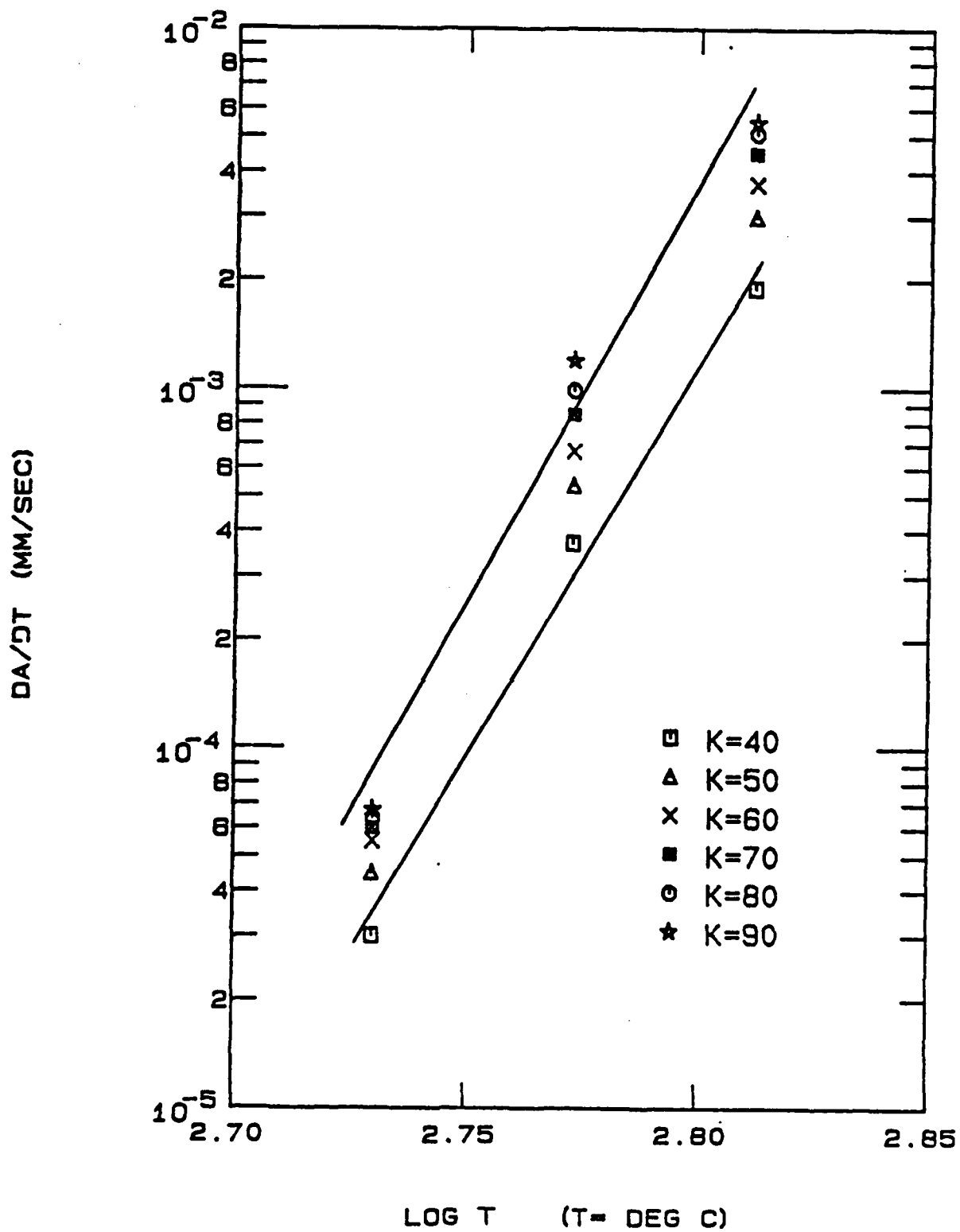


Figure 6. Crack Growth Rate vs Temperature for the Isothermal Baselines

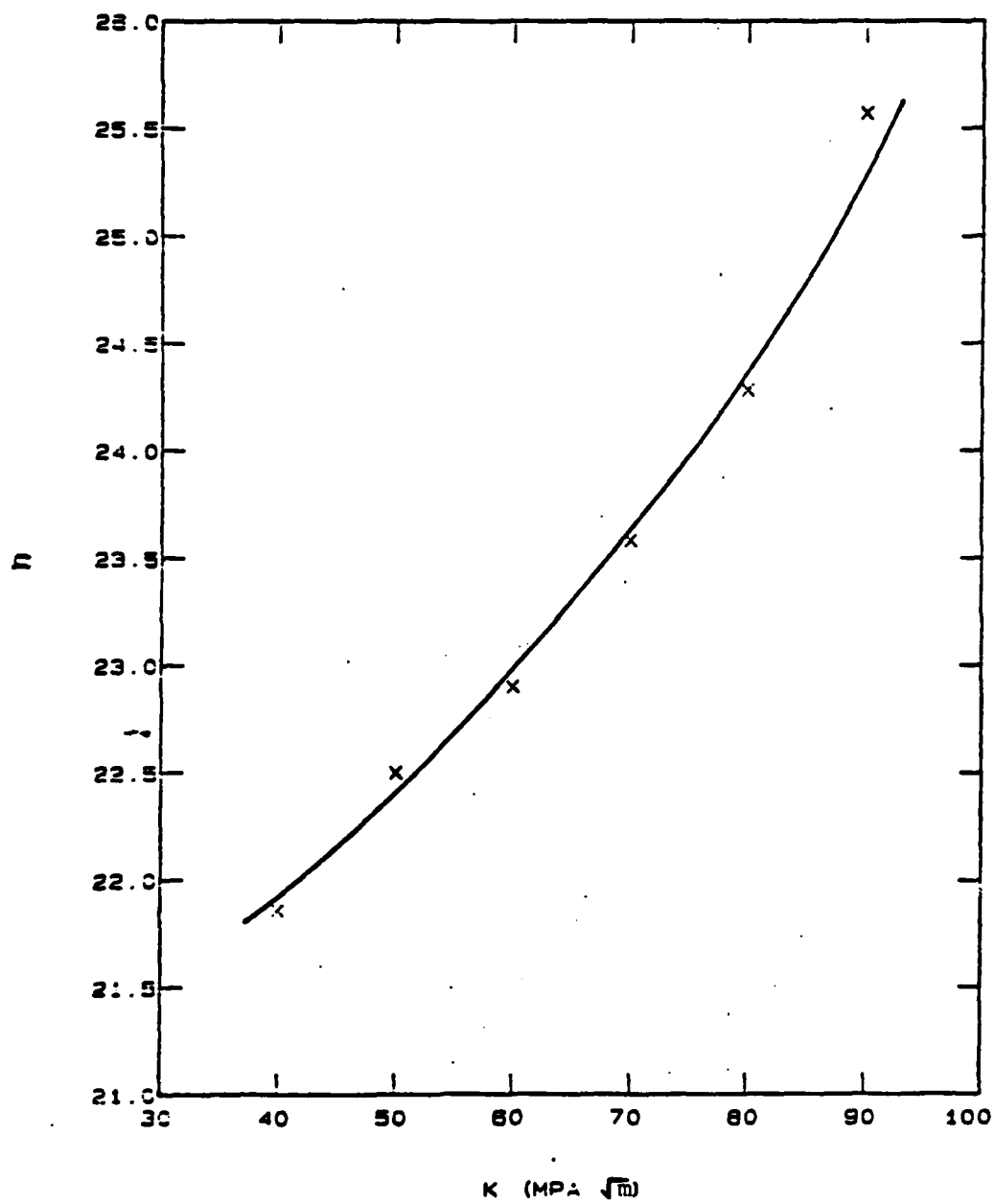


Figure 7. Slope (n) of da/dt vs T Curves Plotted Versus K

fall along straight lines on this log-log scale. Each line has a different slope. Thus, for any constant K value, the crack growth rate can be written as a function of temperature in the form:

$$da/dt = CT^n \quad (1)$$

Here

da/dt = crack growth rate (mm/sec)
 C = intercept on the da/dt axis
 n = slope of the da/dt vs T line
 T = temperature (deg C)

Next, a plot of n vs K is obtained from Fig 6, by determining the slope n at various K values. This n vs K curve is shown in Fig 7.

The temperature is controlled during the tests and it varied linearly with time as shown in Fig 8. Using this figure, the temperature T may be expressed as a linear function of time given by

$$T = T_1 + (T_2 - T_1)(t - t_1)/(t_2 - t_1) \quad (2)$$

Substitution of Eq 2 into Eq 1 leads to an expression for the crack growth rate as a function of time.

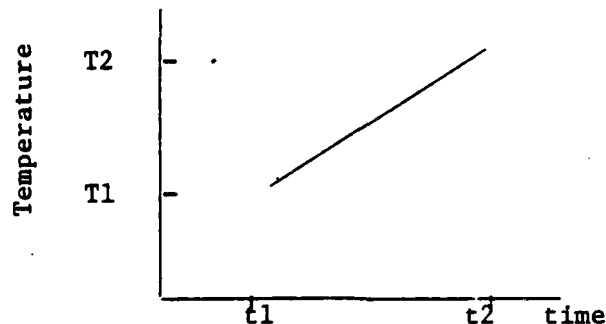


Figure 8. Linear Temperature Variation with Time

$$da/dt = C[T_1 + (T_2 - T_1)(t - t_1)/(t_2 - t_1)]^n \quad (3)$$

Multiplying both sides of Eq 3 by dt and then integrating both sides yields an expression for the change in crack length due to the change in temperature from T1 to T2.

$$\Delta a = a_2 - a_1 = C \left\{ [T_1 + (T_2 - T_1)(t - t_1)/(t_2 - t_1)]^{n+1} (t_2 - t_1) \right\} / (n+1)(T_2 - T_1) \Big|_{t_1}^{t_2} \quad (4)$$

Assuming the test starts at time equal to zero ($t_1=0$), the total time required for the temperature change to occur is t_2 . The average change in crack growth rate is obtained by dividing both sides of Eq 4 by the total time t_2 .

$$\Delta \dot{a}_{ave} = C [T_1 + (T_2 - T_1)(t)/t_2]^{n+1} / (n+1)(T_2 - T_1) \Big|_0^{t_2} \quad (5)$$

Here

$$da/dt = \dot{a}$$

After evaluating the above expression at the limits of integration, the change in crack growth rate is now only a function of n, C, and the temperature limits T1 and T2.

$$\Delta \dot{a}_{ave} = C(T_2^{n+1} - T_1^{n+1}) / (n+1)(T_2 - T_1) \quad (6)$$

Using Eq 1, equation 6 may be written in the form

$$\Delta \dot{a}_{ave} = [(\dot{a}_{T_2})(T_2) - (\dot{a}_{T_1})(T_1)] / (T_2 - T_1)(n+1) \quad (7)$$

This gives the average change in crack growth rate as a function of the isothermal baseline crack growth rates, \dot{a}_{T_1} and \dot{a}_{T_2} . Note that this expression shows that \dot{a}_{ave} is independent of the intercept C and of the

time t_2 , the time required to accomplish the temperature change. Thus, the rate, at which the temperature is changed, does not affect the predicted crack growth rate. As it will be seen later, this condition is verified by the Type 1 test results.

For a temperature profile, such as the one shown in Fig 9, the predicted change in crack growth rate, due to the non-symmetric temperature changes, may be determined using Eq 7.

In this profile, the rate of temperature increase is different than the rate of temperature decrease (t_1/t_2). Using Eq 7 twice, two \dot{a} values were obtained: one for the T_1 to T_2 change, \dot{a}_1 , and one for the T_2 to T_1 change, \dot{a}_2 . These two crack growth rate changes are combined in the following manner to yield the total change in crack growth rate:

$$\dot{a}_{\text{total}} = [(\Delta \dot{a}_1)(t_1) + (\Delta \dot{a}_2)(t_2)] / (t_1 + t_2) \quad (8)$$

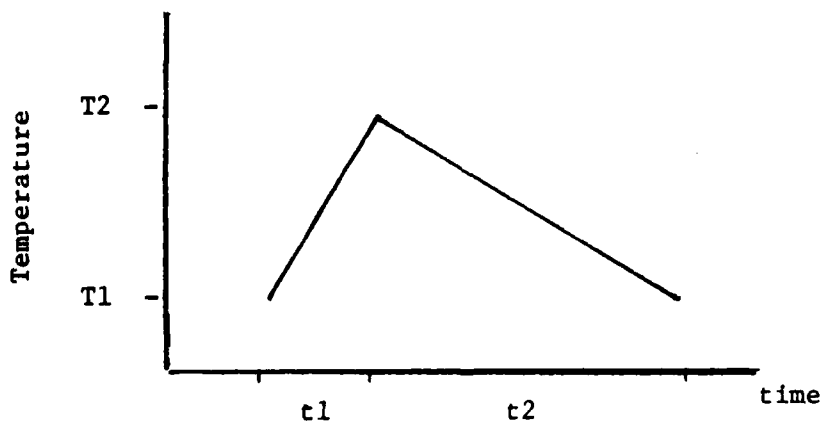


Figure 9. Temperature Cycle with No Hold Time

As discussed previously, the change in crack growth rate is independent of the rate of temperature change; therefore, $\Delta \dot{a}_1$ must equal $\Delta \dot{a}_2$. Substitution of this equality into Eq 8 leads to the following:

$$\Delta \dot{a}_{\text{total}} = \Delta \dot{a}_1 = \Delta \dot{a}_2 \quad (9)$$

Thus, the predicted crack growth rate, \dot{a}_{pred} , resulting from changing the temperature from T_1 to T_2 and back to T_1 , is obtained by adding the isothermal baseline crack growth rate to the $\Delta \dot{a}_{\text{total}}$ of Eq 8:

$$\dot{a}_{\text{pred1}} = \dot{a}_{T1} + [(\dot{a}_{T2})(T_2) + (\dot{a}_{T1})(T_1)] / (T_2 - T_1)(n+1) \quad (10)$$

The subscript 1 refers to Type 1 testing as described in Table II.

When hold times are included in the cycle, such as the one shown in Fig 10, equation 10 is modified to include the effect of the hold time, t_4 :

$$\dot{a}_{\text{pred2}} = [(\dot{a}_{\text{pred1}})(t_3) + (\dot{a}_{T1})(t_4)] / (t_3 + t_4) \quad (11)$$

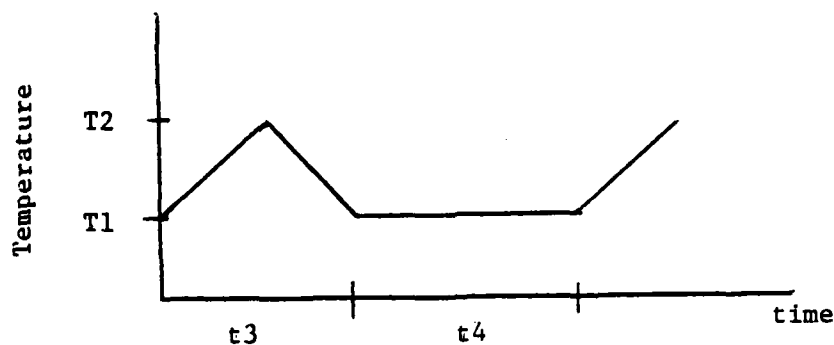


Figure 10. Temperature Profile with Hold Time

Recall that the subscript 2 refers to Type 2 tests (see Table II). The crack growth rate for a cyclic temperature variation with hold times is predicted using Eq 11.

To predict the rate of crack growth for the tests which include hold times (Test Types 2, 3, and 4), Eq 11 is modified by adding the appropriate amount of hold time. This predicts the crack growth rate for a specific K value. By repeating the process for several K values, the entire da/dt vs K curve can be plotted. An example of this procedure appears at the end of this section.

This prediction model may be applied to more complex temperature profiles. A proof test, with the temperature profile, shown in Fig 11, was conducted to verify the model for a more complex situation. Non-symmetric temperature profiles, such as this, are representative of actual mission profiles. It should be noted that $t_1 \neq t_3$ and that $t_2 \neq t_4$; that is, the rates of temperature increase and decrease are different as well as the hold times at the high and low temperatures. This profile was continuously repeated until failure occurred.

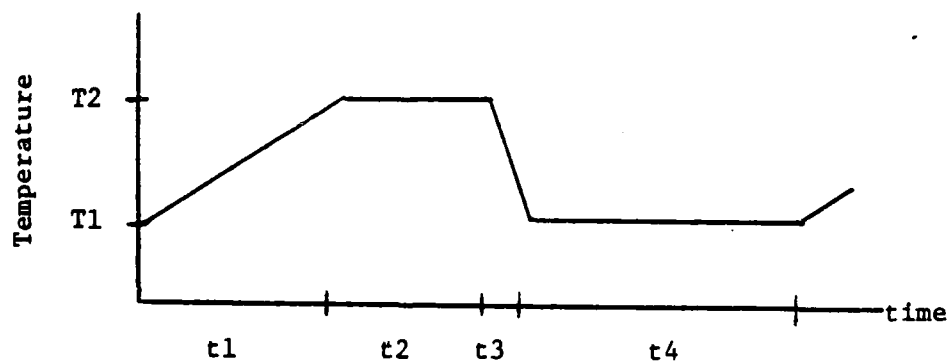


Figure 11. Non-symmetric Temperature Profile of the Proof Test

Modifications to Eq 11 must be made in order to predict the crack growth rate for the proof test. The rate of temperature increase has been combined with the rate of temperature decrease to form \dot{a}_1 as shown in Eq 8. Thus, the total crack growth rate for the proof test is predicted by:

$$\dot{a}_{pred3} = [(\dot{a}_1)(t1+t3) + (\dot{a}_{T2})(t2) + (\dot{a}_{T1})(t4)] / (t1+t2+t3+t4) \quad (12)$$

It should be noted that any transient effects due to changing temperatures, or any history effects from cycle to cycle, have not been included in this prediction. That is, the equations used for predicting crack growth rates assume that each temperature loading cycle is independent of the preceding cycles. One of the purposes of this investigation is to examine the consequences of ignoring these effects. They are known to exist, but neglecting their contribution to the crack growth rate simplifies the model considerably. An estimate of the error introduced by not accounting for these effects is obtained by comparing predictions to the actual experimental results. This is done in the Experimental Results and Discussion section.

To illustrate the use of Eq 12, consider the following example.

The proof test, specimen number 81-240W, used the temperature profile given in Fig 11. The actual test parameters are shown below.

T1 = 537C	t1 = 66 sec
T2 = 648C	t2 = 60 sec
	t3 = 24 sec
	t4 = 180 sec

As shown earlier, the rate of temperature increase may be combined with the rate of decrease to form a crack growth rate calculated by Eq 8.

$$\dot{a}_{\text{pred1}} = \dot{a}_{537} + [(\dot{a}_{648})(648) + (\dot{a}_{537})(537)] / (648 - 537)(n+1) \quad (13)$$

This growth rate, resulting from the two changes in temperature, is added to the crack growth rates resulting from the two hold times. This is accomplished using Eq 12, modified to allow for the additional hold time.

$$\dot{a}_{\text{pred3}} = [(\dot{a}_{\text{pred1}})(90) + (\dot{a}_{648})(60) + (\dot{a}_{537})(180)] / 330 \quad (14)$$

Using the isothermal baselines (Fig 5), \dot{a}_{648} and \dot{a}_{537} are determined for various K values. Values for n are obtained in the same manner using Fig 7. Substituting these values into Eq 12 and Eq 13, in turn, produces the predicted crack growth rate \dot{a}_{pred3} for a specific K value. By repeating the procedure for various K values, a predictive plot of da/dt vs K can then be made. The predicted crack growth rate curve for the proof test as well as the actual test results, are shown in Fig 19. To illustrate the above procedure consider

$$K = 40 \text{ MPa(m)}^{1/2}$$

then, the following results are obtained

$$\begin{aligned} n &= 21.86 \text{ (from Fig 7)} \\ \dot{a}_{537} &= 3.1 \times 10^{-5} \text{ mm/sec (from Fig 5)} \\ \dot{a}_{648} &= 2.0 \times 10^{-3} \text{ mm/sec (From Fig 5)} \end{aligned}$$

Substitution of these values first into Eq 12 and then into Eq 13 leads to a prediction for the crack growth rate for the proof test at $K = 40 \text{ MPa(m)}^{1/2}$:

$$\dot{a}_{\text{pred,proof}} = 5.18 \times 10^{-4} \text{ mm/sec} \quad (15)$$

The time-to-failure for the proof test is predicted next. This

is done by making use of the predicted crack growth rate curve plotted in Fig 19. Note that the error obtained between the predicted crack growth rate and the actual test results will be carried over to the prediction for the time-to-failure.

It was decided that when the stress intensity factor (K) reached a value of $80 \text{ MPa(m)}^{1/2}$ the specimen was considered to have failed. This K value at failure is converted to crack length at failure (a_f) by using the appropriate equation for center cracked specimens:

$$K = \sigma(\pi a)^{1/2} (\sec \pi a/W)^{1/2} \quad (16)$$

For the specimen geometry and test conditions used in this investigation (Tables I and III), the crack length at failure is calculated to be 15.494 mm. The time-to-failure t_f may be represented as

$$t_f = \int_0^{t_f} dt = \int_{a_0}^{a_f} da / (da/dt) \quad (17)$$

Recall that Eq 1 expresses da/dt in terms of K:

$$da/dt = CK^n \quad (\text{restated}) \quad (1)$$

Also, K can be written as a function of crack length (a) as given by Eq 16. Combining Eqns 1, 16, and 17 a linear cumulative model is obtained for predicting the time-to-failure in terms of crack length:

$$t_f = 1/C \int_{a_0}^{a_f} [\sigma (\pi a)^{1/2} (\sec \pi a/W)^{1/2}]^{-n} da \quad (18)$$

Here, C and n are determined by dividing the predicted crack growth rate curve given in Fig 19 into two portions, each of which is very close to being linear. Assuming that they are linear, the slopes of each line are the values for n, and the intercepts on the da/dt axis are the values for C. The integration of Eq 18 was done numerically, once for each linear portion of the predicted da/dt vs K curve of

Fig 19. The calculated values of n and C , and the actual test parameters are substituted into Eq 18. The numerical integration was performed using a standard trapezoidal integration computer routine. Time-to-failure was predicted to be 10,225 seconds. Actual test time-to-failure ($K = 80 \text{ MPa(m)}^{\frac{1}{2}}$) was 18340 seconds, which represents 44 percent error.

As mentioned earlier, some of this error may be due to the error in the predicted crack growth rate curve. This will be discussed further in the Experimental Results and Discussion section.

V Experimental Results and Discussion

The experiments described in the experimental procedures section (Chapter III) were performed using the facilities of the US Air Force Wright Aeronautical Laboratories (Materials Laboratory). The results obtained from these experiments are presented and discussed in this chapter. The raw test data appear in Appendix C in free-format form. Unless otherwise stated, the temperature was changed at a rate of 4.625C/sec. Arrows which appear above or below the crack growth rate curves (da/dt vs K) signify overnight test shutdowns. The temporary retardation in the crack growth rate caused by these overnight shutdowns was disregarded during the curve fit.

The isothermal baseline data were gathered for three temperatures: 648, 593, 537C. These data and corresponding curve fits are presented in Fig 4. The procedures for gathering and reducing the baseline data are presented in Chapter III. Only the isothermal baselines are presented in Fig 5. These lines were used to predict the crack growth rates for the non-isothermal tests.

The transition time tests were used to determine the time required for the crack growth rate to return to its isothermal baseline rate after the temperature was changed. The transition times were obtained by comparing the raw data and the crack growth rate curves of the isothermal baselines to the data and crack growth rate curves of the transition tests. This investigation did not require an exact transition time.

The data for the first transition test, specimen number 81-246, is

plotted in Fig 12. The test began with the temperature at 648C for 1410 seconds. The temperature was then decreased to 537C and held there for 63510 seconds. Finally, the temperature was raised to 593C and held until failure occurred. It is seen that raising the temperature from 537C to either 593C or to 648C has no noticeable effect upon the crack growth rate. The slope of the crack growth rate curve is essentially the same as the slope of the isothermal baseline rates. However, when the temperature was lowered from 648C to 537C, the crack growth rate is retarded. From the raw data, zero crack growth was observed for nearly 3 minutes after the temperature was lowered and stabilized. The time required for the crack growth rate to return to the 537C baseline rate was nearly 55 minutes.

Test specimen number 81-247 was tested to determine the approximate transition time after the temperature is lowered to 593C from 648C. The results are depicted in Fig 13. The test began at 648C for 1740 seconds. The crack growth rate here closely follows the slope of the 648C isothermal baseline rate. The temperature was decreased to 593C and held for 8030 seconds. During this time, zero crack growth occurred for nearly 1.5 minutes, as indicated by the raw test data. It took approximately 49 minutes for the crack growth rate to stabilize at the 593C isothermal baseline rate. When the temperature was raised again to 648C, no difference was observed between the slope of this growth rate and the slope of the 648C isothermal baseline rate.

Continuous cycle tests were conducted with no hold times (Type 1). Three different temperature change rates were used:

- (a) 4.625C/sec; yielding a 48 sec cycle

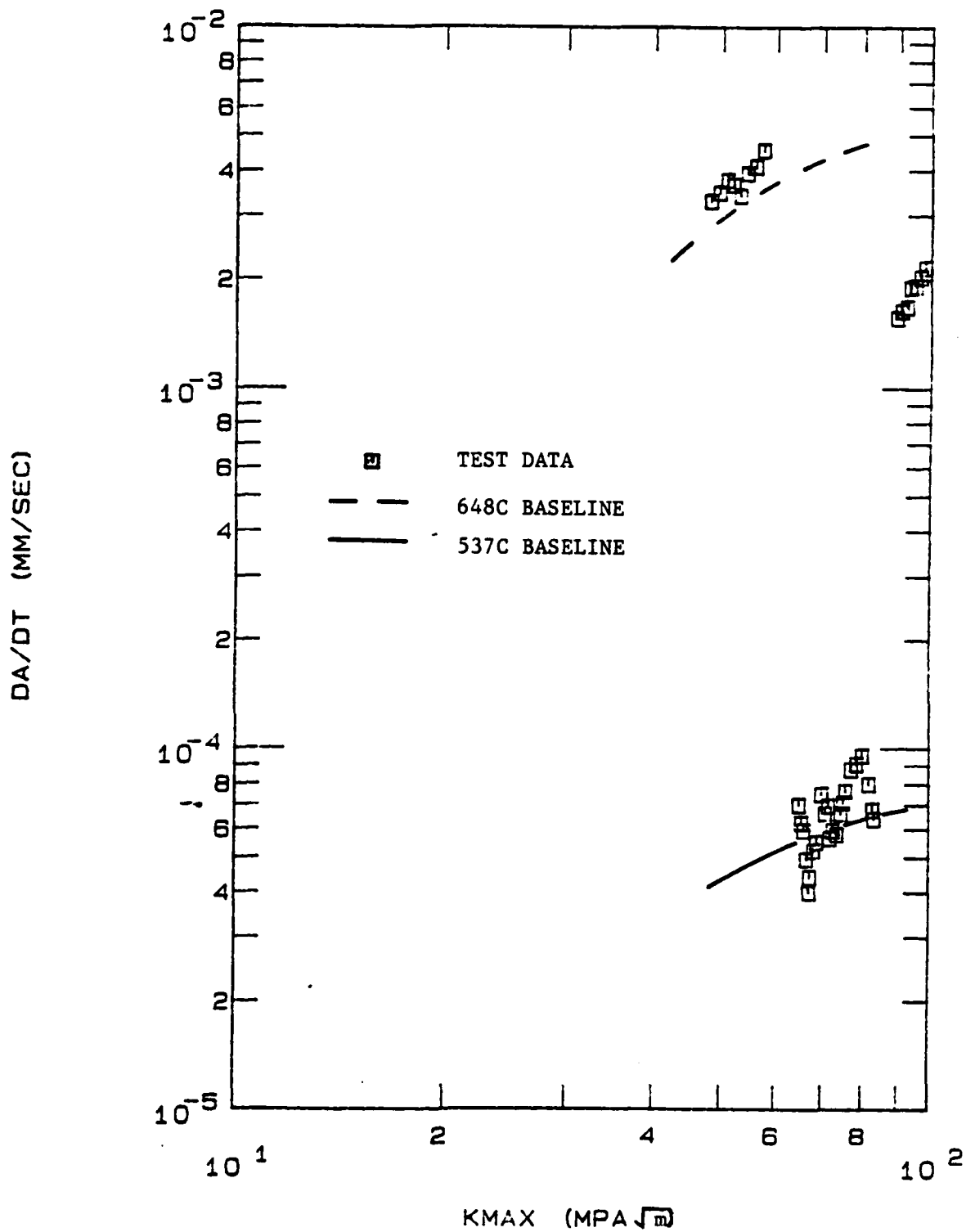


Figure 12. Transition Crack Growth Rate for Specimen 81-246 from 648C to 537C to 593C

DA/DT (MM/SEC)

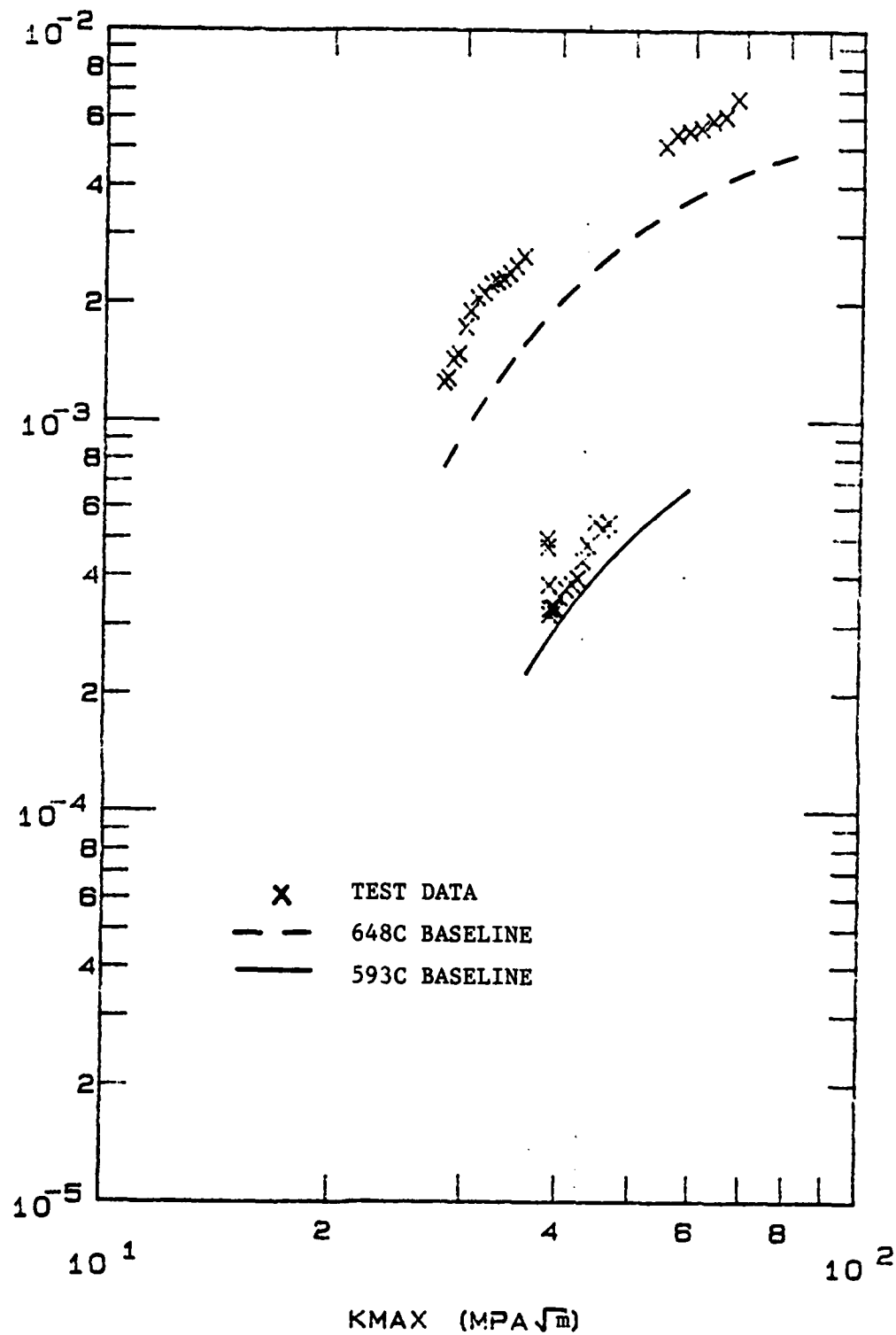


Figure 13. Transition Crack Growth Rate for Specimen 81-247 from 648C to 593C to 648C

(b) 1.680C/sec; yielding a 132 sec cycle

(c) 0.4625C/sec; yielding a 480 sec cycle

Two tests were conducted for each rate. The data for each pair of tests per temperature change rate were averaged into one curve. The data and curve fit, of each temperature change rate, are shown in Appendix B. When these curves are all depicted on one plot, as shown in Fig 14, it is seen that the data of all six tests fall within the normal scatter range of similar tests (10). This verifies that the crack growth rate is independent of the rate of temperature change. The three individual curves, one for each temperature change rate, were averaged into one curve using a polynomial regression curve fit. The average curve, shown as a solid line in Fig 14, was compared to a french curve fit of the same data. There was very little error between the two curve fits. This average curve for the Type 1 tests is compared to the predicted crack growth rate curve obtained from the model outlined in Chapter IV. This comparison is shown in Fig 15.

It is seen in Fig 15 that the model predicts a higher crack growth rate at the beginning of the test than what was observed. The largest difference is 0.8×10^{-4} mm/sec at the beginning of the test. This represents an error of 44.5 percent. However, as the test continues, the prediction converges toward the experimental results. At specimen failure, there is almost no difference between the predicted and the actual crack growth rates. This region of negligible error corresponds to a crack growth rate of 1×10^{-3} mm/sec. Thus, for the Type 1 tests, the predictions were more accurate at the higher crack growth rates.

It is interesting to note that the data for both tests conducted at

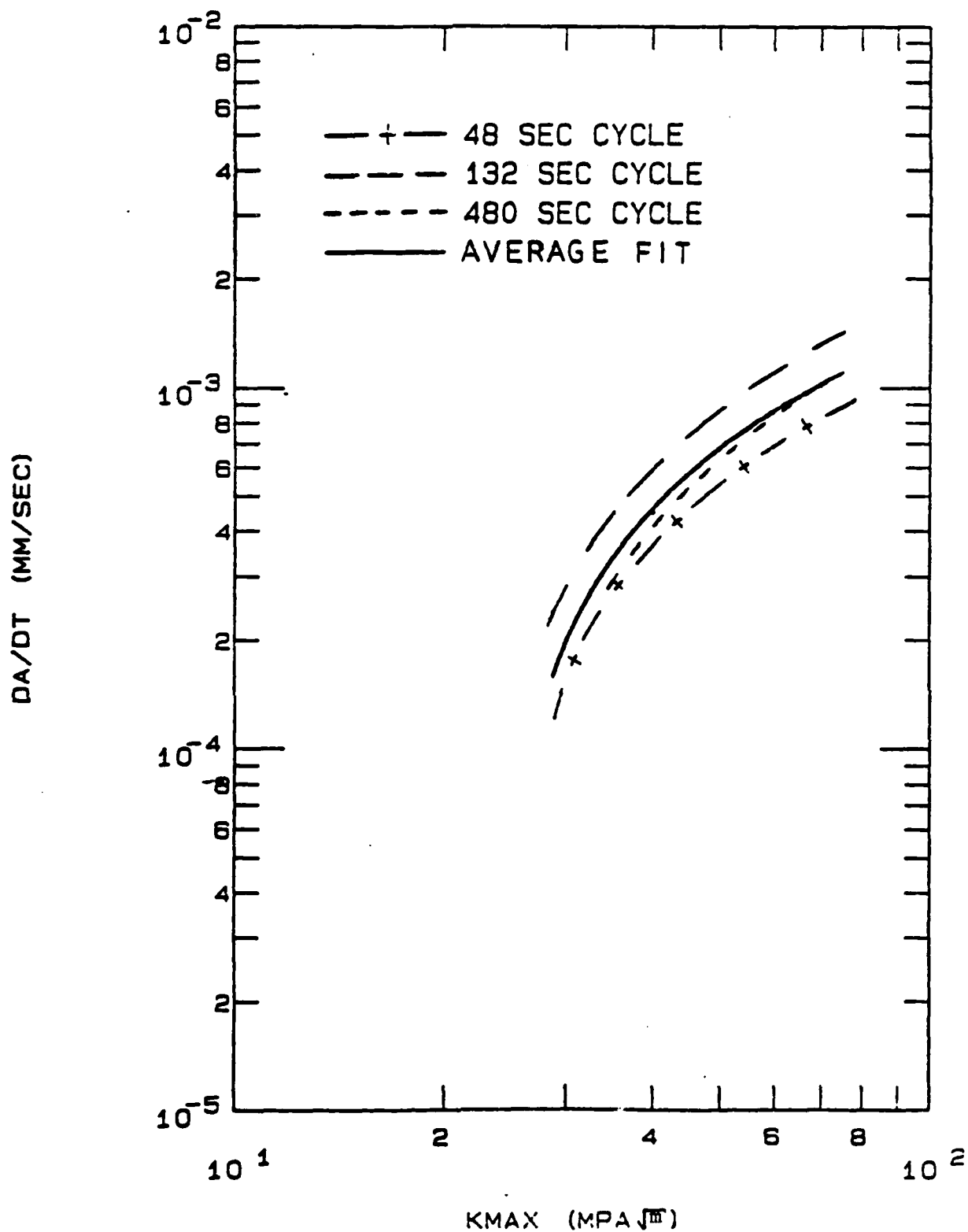


Figure 14. Individual Type 1 Crack Growth Rates for Various Temperature Change Rates Compared to the Average of All Data

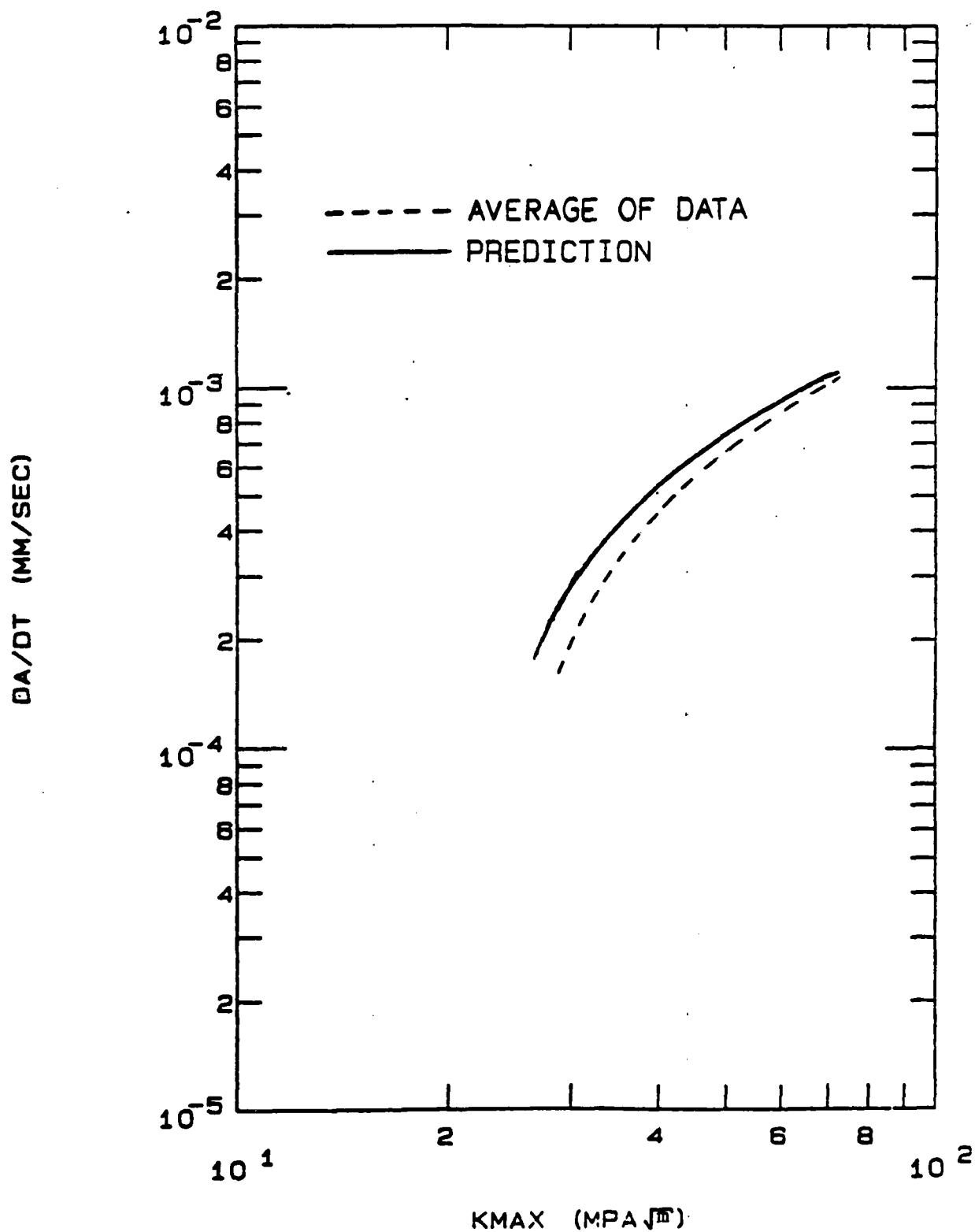


Figure 15. Type 1 Prediction Compared to the Average of all Type 1 Data

the fastest rate of temperature change (4.625C/sec; 48 sec cycle) are extremely close to the data for the 593C isothermal baseline (see 48 sec cycle curve in Appendix B). When the temperature is cycled at this rapid rate between 648C and 537C, the crack growth rate seems to simply be the average of the rates at the two extreme temperatures. Any retardation effects and crack resharping seem to have no chance to take effect.

The results of the Type 2 test are compared to the corresponding predicted crack growth rate curve in Fig 16. In this test, temperature is held for 3 minutes at 648C, and then decreased to 537C with no hold time, and finally increased back to 648C. Throughout this test, the crack growth rate was high (above 1×10^{-3} mm/sec), and the model produced very accurate predictions.

Two different hold times (3 and 15 minutes) were used during the Type 3 tests. Here, the temperature was held at 537C and then raised to 648C, and immediately returned to 537C. This cycle was repeated until the specimens failed. The results of the 3 minute hold time test are compared to the predicted crack growth rate in Fig 17. For this case, the model gives a conservative prediction. There is an almost constant difference of 1×10^{-4} mm/sec between the prediction and the experimental results. The prediction is within a factor of two of the experimental results. This test produced a slow crack growth rate (approximately 1×10^{-4} mm/sec) and the error is larger. The error, though, is within the range of scatter obtained during other testing at similar conditions.

The results of the 15 minute hold time test are compared to the

DA/DT (MM/SEC)

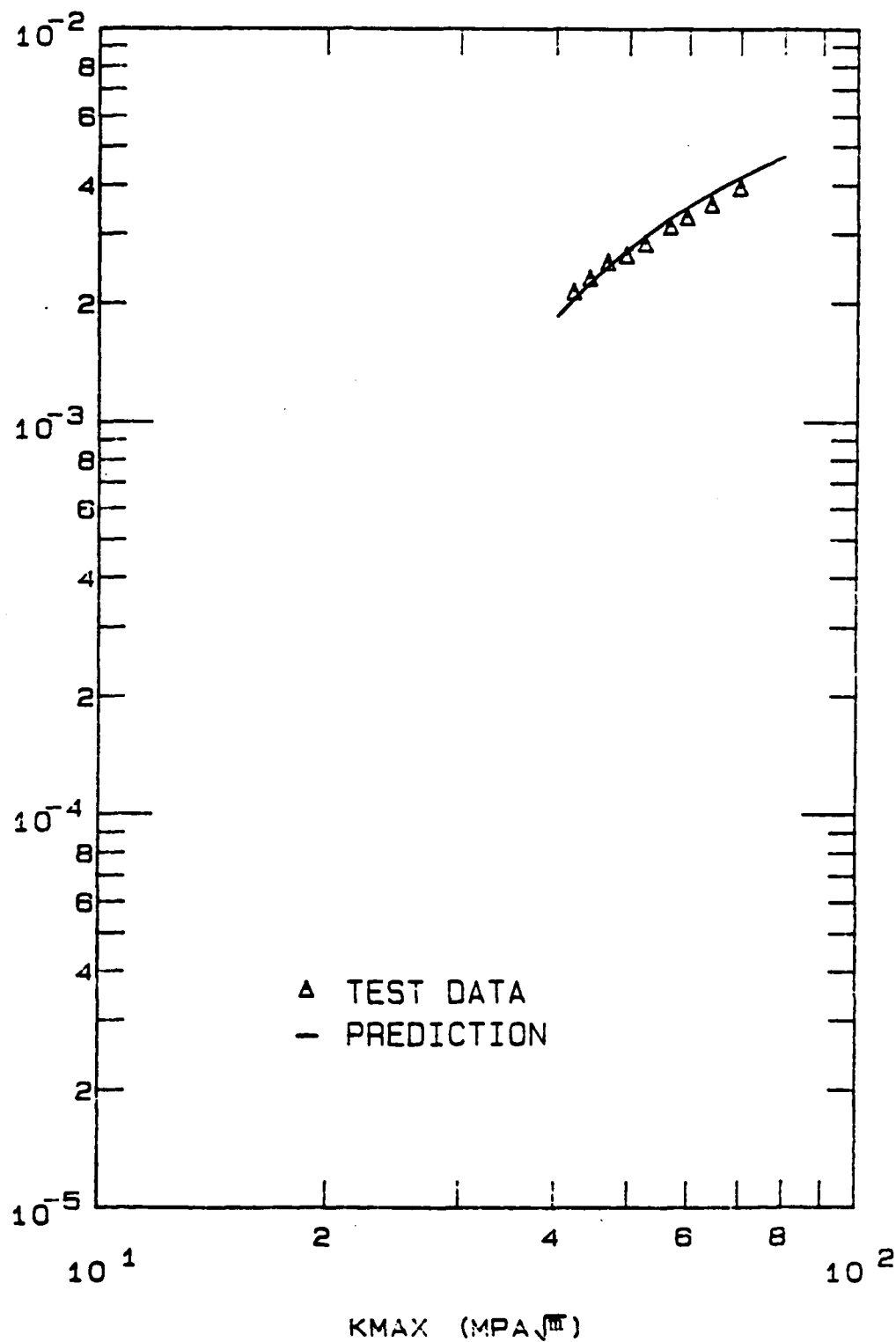


Figure 16. Test Data and Prediction for Type 2 Test With a 3 Minute Hold Time

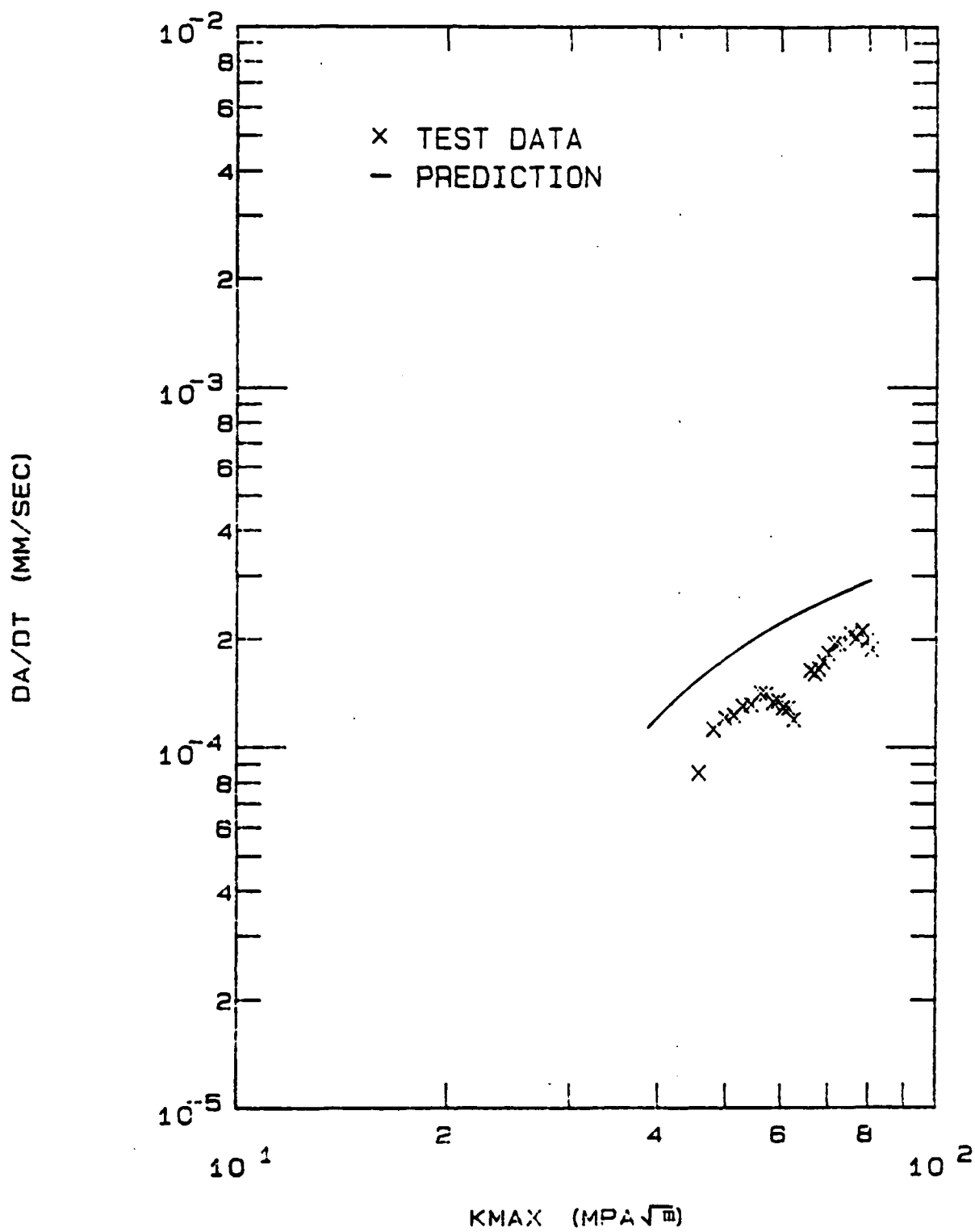


Figure 17. Prediction and Data for the Type 3 Test with a 3 Minute Hold Time

predicted crack growth curve in Fig 18. Note that the model predicted a slower crack growth rate than that achieved from the experiment. Here again the difference is within the scatter range of a factor of two.

Comparing the 3 minute hold time test results to the test with the 15 minute hold time, indicates almost identical crack growth rates. This suggests that the time rate of crack growth (da/dt) is the same for any stress intensity factor (K). Multiplication of da/dt by the time per cycle produces the crack growth per cycle (da/dn). The da/dn vs K curves for the 0, 3, and 15 minute hold time tests are shown in Fig 19. The time per cycle differs approximately by a factor of four between the three tests. This indicates that the crack growth per cycle should also differ approximately by a factor of four, if the time rates of crack growth were indeed equal. As seen in Fig 19, the crack growth per cycle curves (da/dn) do not differ by a factor of four. The difference between the curves becomes greater as the amount of hold time increased. Therefore, the crack growth rate (da/dt) is dependent upon the amount of hold time at 537C. Even though crack growth was temporarily retarded during the transition tests after a decrease in temperature, the growth rate at 537C seems to have a positive contribution to the overall crack growth rate for the test. The contribution becomes larger as the hold time is increased.

The linear model accurately predicts the crack growth rates for each of the Type 4 tests. In these tests, the same hold time is used both at 648C and 537C. One test used a 3 minute hold time and the second test used a 15 minute hold time. The linear model predicted

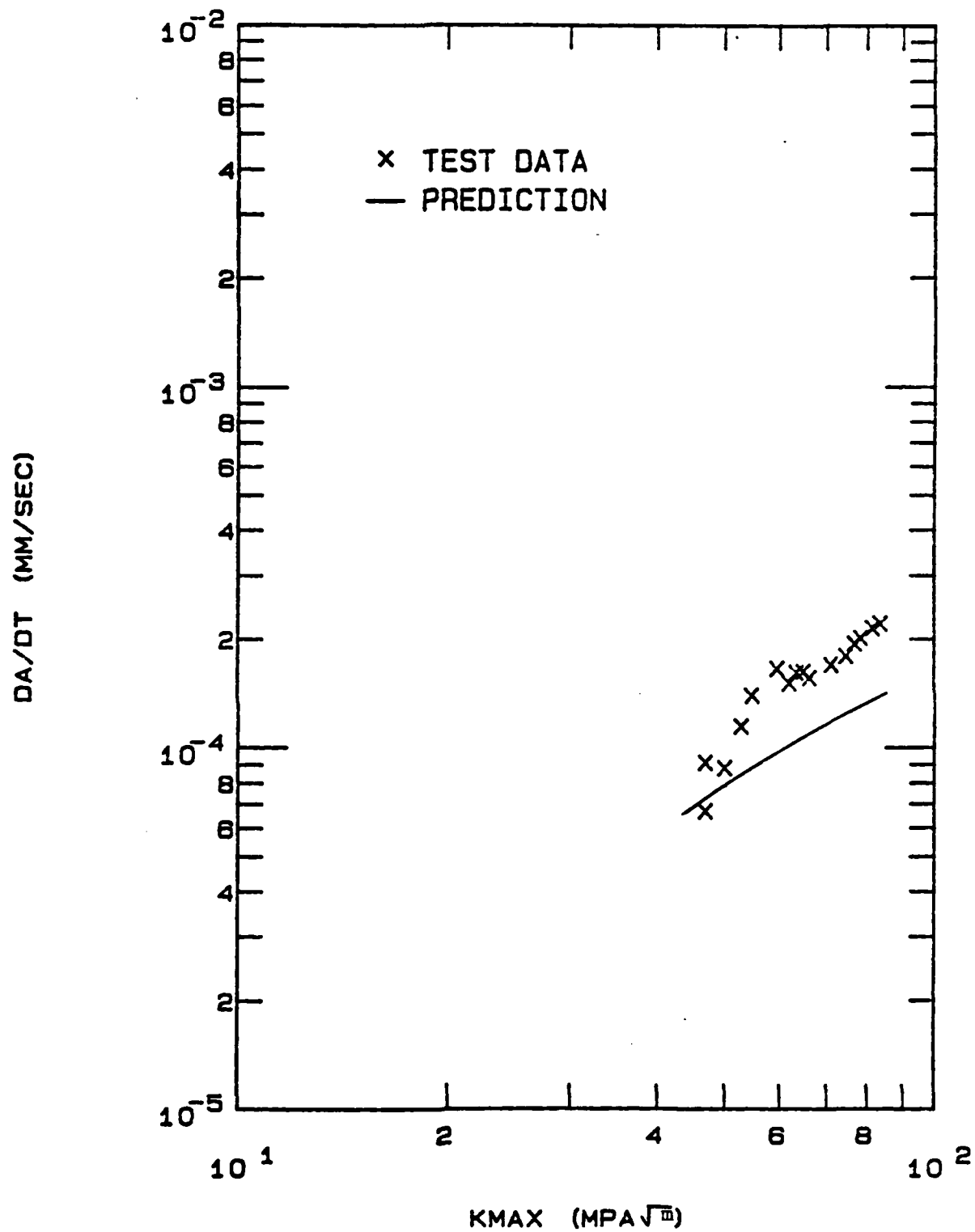


Figure 18. Prediction and Data for the Type 3 Test with a 15 Minute Hold Time

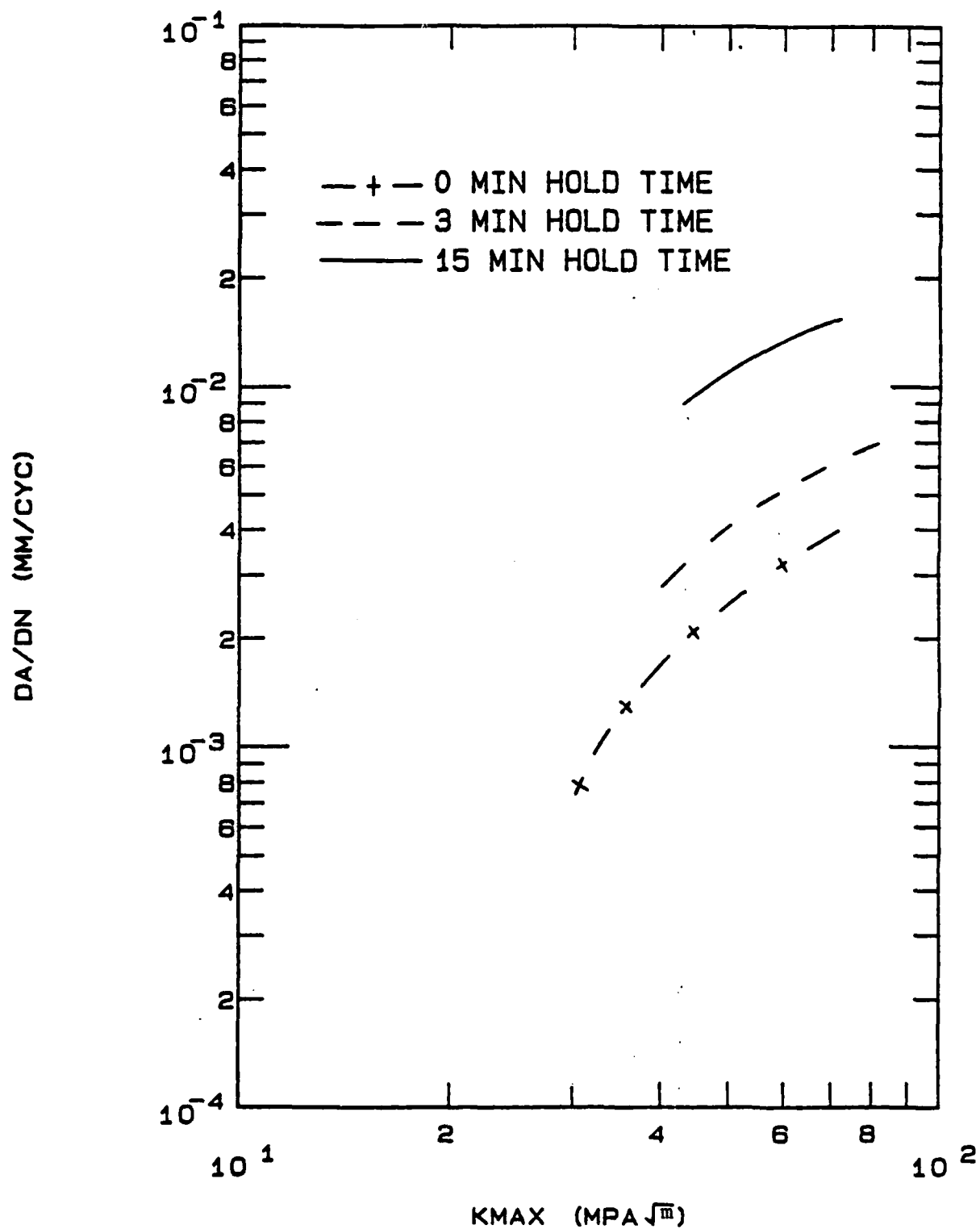


Figure 19. Crack Growth per Cycle for Type 3 Tests

very similar crack growth rates for the two tests. The two predictions are plotted as one curve in Fig 20, since they are so close. The test using the 15 minute hold time differs the most from the prediction. Here again, this difference is well within the experimentally observed scatter range. These tests produced a moderate crack growth rate, $(0.5 \text{ to } 1) \times 10^{-3}$ mm/sec, and the linear model's predictions were accurate.

A proof test was conducted to verify the predictions of the linear model for a more complex temperature profile. In this test, a different rate is used for increasing the temperature than the one used for decreasing it. Also, the hold time at 648C does not equal the hold time at 537C. The experimental results of this test are compared to the prediction in Fig 21. In this test the crack growth rate ranged from moderate to fast. It should be noted that the prediction improves as the crack growth rate increases. The largest error, 2×10^{-4} mm/sec, occurs at the beginning of the test and is approximately 71 percent. As the test continues, the prediction converges to the experimental results. Close to the failure point, the crack growth rate is near 1×10^{-3} mm/sec and the error is negligible. Thus, the linear model accurately predicts the crack growth rate for this complex temperature profile.

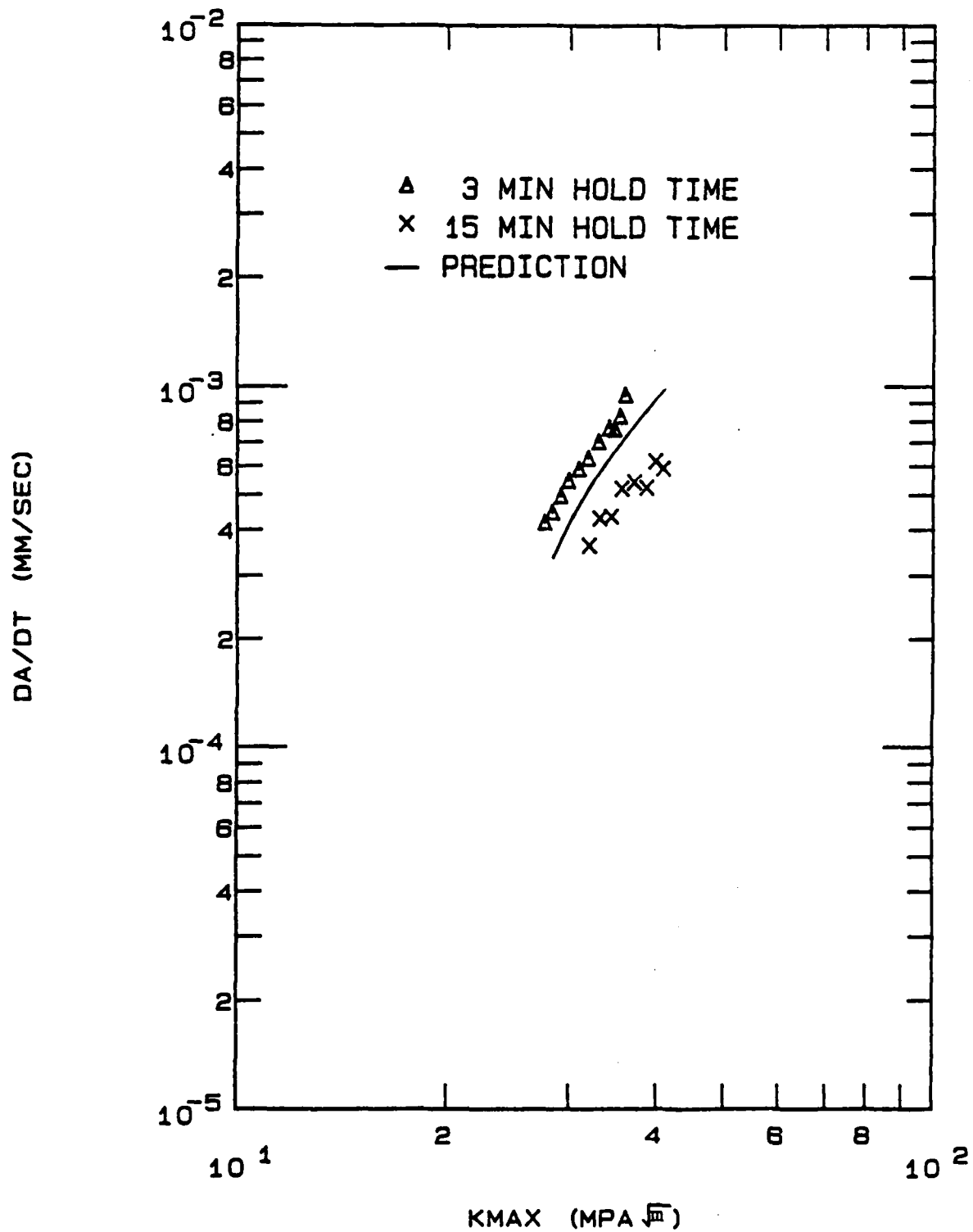


Figure 20. Prediction and Data for Both Type 4 Tests

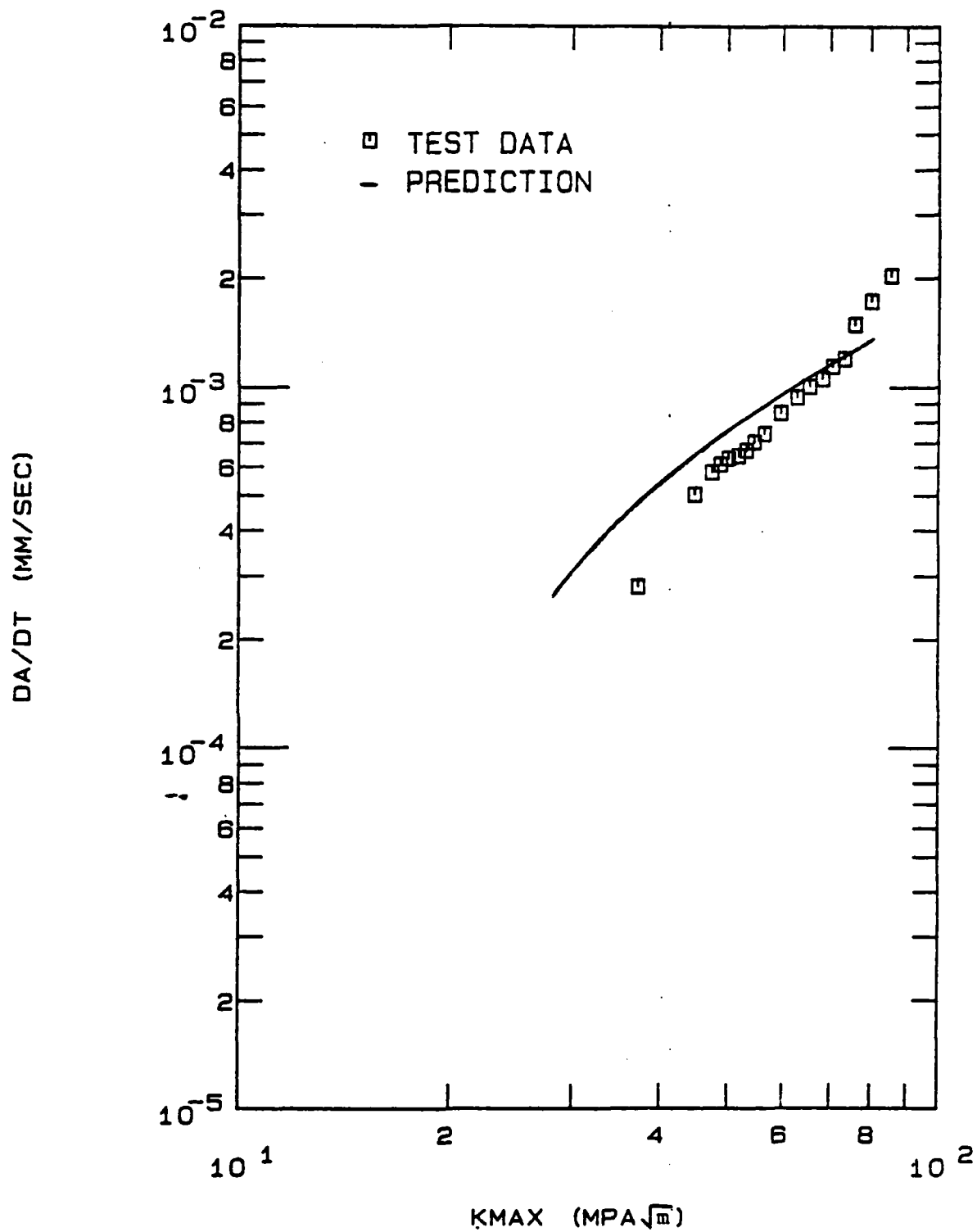


Figure 21. Data and Prediction for the Proof Test

VI Conclusions and Recommendations

Conclusions

Within the scope of this investigation, linear cumulative damage modeling accurately predicts creep crack growth rates under non-isothermal conditions. All of the predictions were within a factor of two of the experimental results. This is within the range of experimental scatter observed throughout this project. Therefore, the impact of ignoring interaction effects and transient effects for continuous temperature cycling appears to have a negligible effect upon the predicted creep crack growth rate. This is true for the temperature range and other limits of this investigation.

Generally, the predictions are conservative. The linear model, in all cases except two, predicted a faster crack growth rate than that produced during the actual test. Therefore, within the scope of this investigation, using the predicted crack growth rates will yield a safe design. It was also shown that by using the predicted crack growth rate, the time-to-failure is accurately predicted.

The linear damage model produced better predictions for the faster crack growth rates. The error between the predicted and experimental crack growth rates was negligible in tests which produced crack growth rates near 1×10^{-3} mm/sec or faster. The error increased as the crack growth rate decreased. The error is approximately 50 to 100 percent

when the crack growth rate is near 1×10^{-4} mm/sec. At these slower crack growth rates, environmental effects have more influence. Also, at these slower growth rates, the interaction and transient effects have ample opportunity to affect the crack growth rate. It should be emphasized, however, that even at these low crack growth rates (1×10^{-4} mm/sec) the difference between the experimental and the predicted values is within a factor of two. This is within the normal range of scatter for similar tests (10).

The proposed linear model also produced very good crack growth rate predictions for the more complex temperature profiles. The error obtained for the proof test was consistent with the errors obtained for the other tests which used symmetric temperature profiles.

It may be concluded that the linear cumulative damage model introduced in this thesis, will accurately predict a conservative crack growth rate for non-isothermal conditions, if within the limits of this investigation.

Recommendations

An effort should be made to expand the range of applicability of the model introduced in this thesis. The linear cumulative damage model should be applied to predict experimental results conducted over wider temperature ranges, and at different temperature change rates. Other materials may be investigated. More tests may be conducted using the more complex temperature profiles. Additional transition data should be

gathered to better understand the transient effects produced by larger temperature changes.

Thermal-mechanical testing should be conducted, using linear cumulative damage modeling to predict the damage caused by the creep portion. Combining the separate effects of creep and fatigue should be investigated further.

APPENDIX A

Heat Treatment History of Test Specimens

Anneal at 968C for 1 hour - air cool

Age at 720C for 8 hours - furnace cool to 620C

Hold at 620C for 10 hours

APPENDIX B

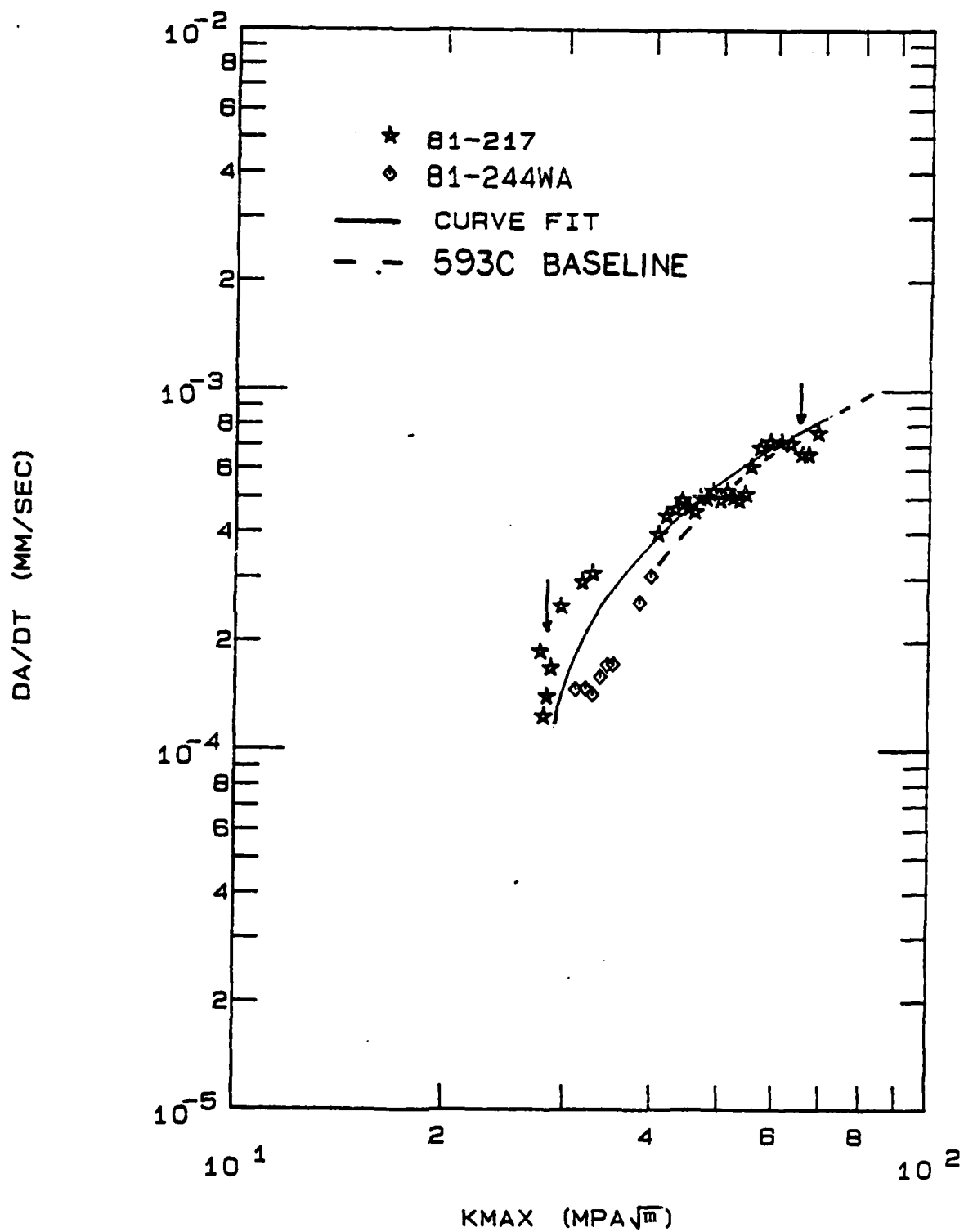
"Crack Growth Rate

versus

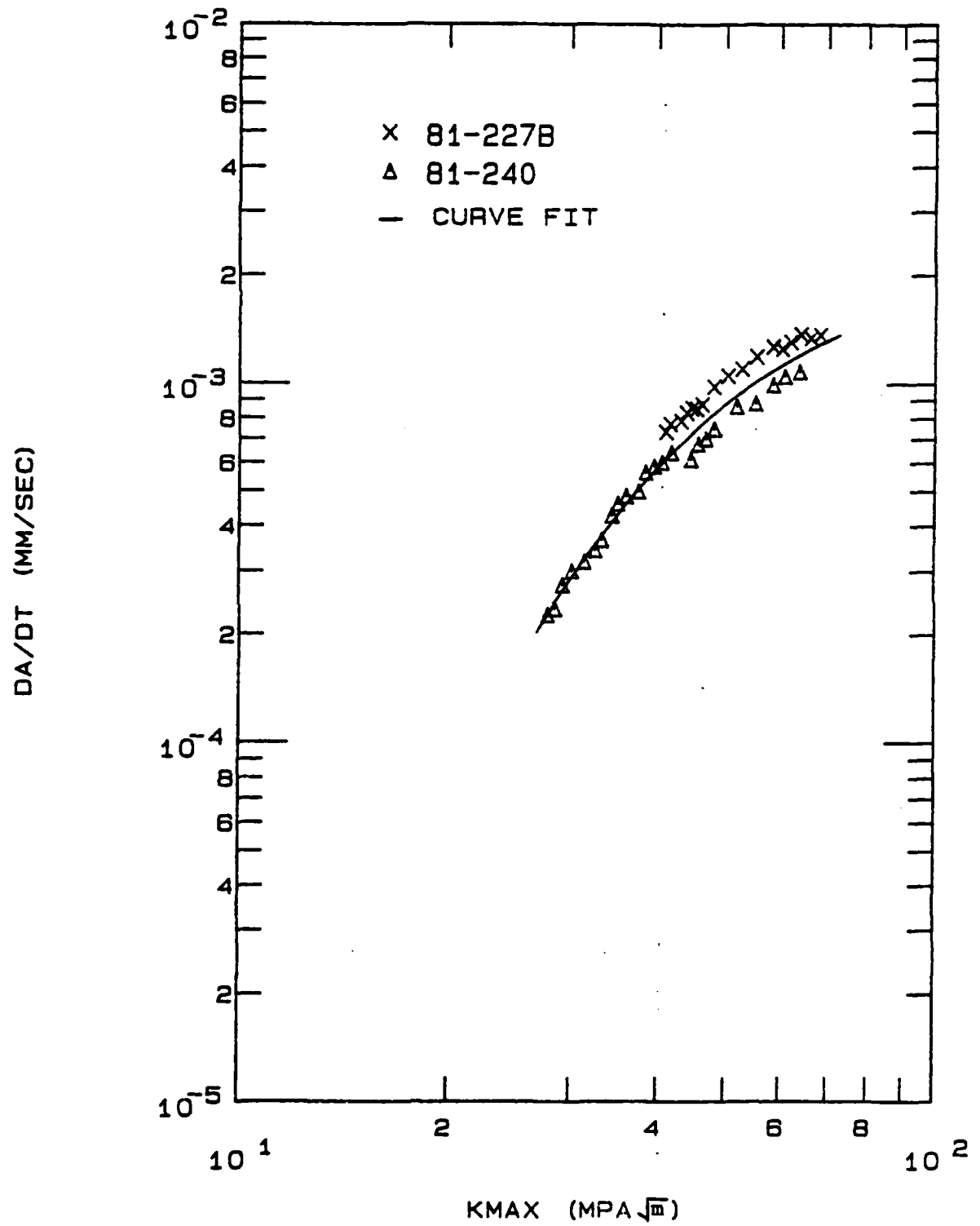
the Stress Intensity Factor" Curves

This Appendix contains the three curves for the individual Type 1 Tests. The first curve is for the two tests conducted with a 48 second cycle and no hold time. Likewise, the second plot is for the data of the two tests conducted with a 132 second cycle. The last plot is for the data of the two tests conducted with a 480 second cycle.

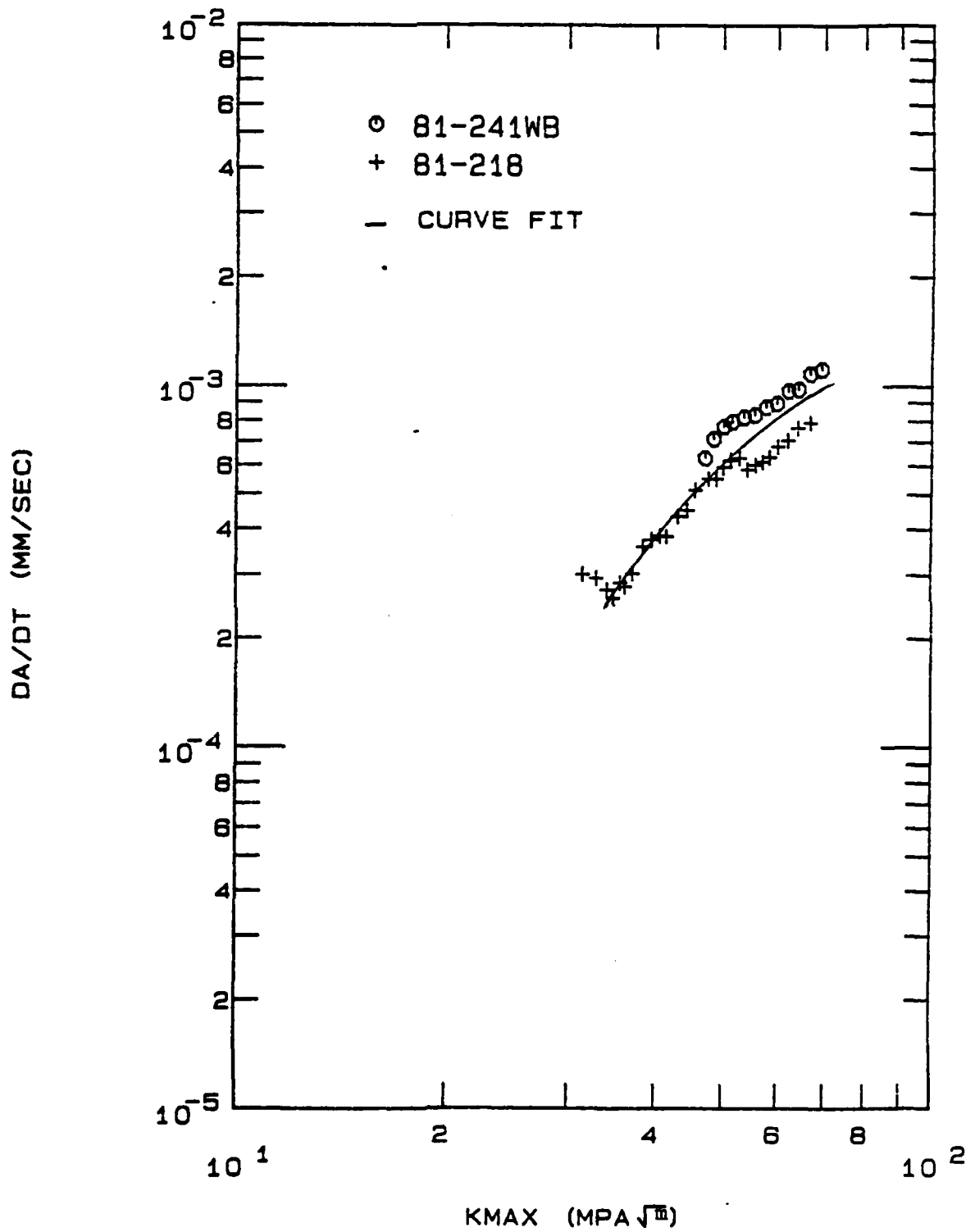
48 SECOND CYCLE



132 SECOND CYCLE



480 SECOND CYCLE



APPENDIX C

Tabulated Raw Test Data

This Appendix contains the raw test data for the tests conducted for this investigation. The data is shown in free-format form. The first value is the time at which the reading was taken, in seconds. The test began at $t=0$. The second value is the crack length, a , where $2a$ is the total crack length. The units of a are inches. The crack length, a , was determined by measuring the location of the crack tip on the right side and subtracting the measurement of the crack tip location on the left side, then dividing by 2.

537C BASELINE DATA

a = half total crack length (inches)
t = total time (seconds)

Specimen
Number
81-244

t	a	t	a
0,.173		175500,.4405	
5000,.178		179100,.4475	
12000,.183		182700,.455	
26940,.1955		188100,.464	
42940,.2149		191700,.471	
79740,.2595		195300,.4825	
90240,.274		198900,.4895	
101100,.293		204000,.504	
104700,.2965		207600,.507	
115800,.313		212100,.515	
117900,.327		216300,.5265	
121500,.328		219540,.540	
125100,.335		225960,.554	
128700,.341		229560,.5615	
132300,.349		233160,.5715	
135900,.3555		236760,.577	
139500,.359		241440,.591	
143100,.370		243840,.598	
146700,.373		247620,.6025	
148680,.383		250200,.6155	
152520,.3915		252900,.621	
155700,.3985		255600,.629	
159300,.405		259200,.6425	
162900,.4075		262800,.648	
164700,.4125		267300,.653	
168300,.4215		271020,.659	
171900,.433		283980,.7005	
		286560,.713	

BASELINE DATA

a = half total crack length (inches)
t = total time (seconds)

537C
Specimen
Number
81-212

t	a
0	.1465
8980	.1535
24200	.172
80100	.2775
87300	.2855
98100	.3115
108900	.3325
122700	.369
129900	.381
140700	.397
147900	.4205
157740	.472
163500	.4765
170700	.484
177900	.502
185100	.528
189540	.5365

593C
Specimen
Number
81-239

t	a
0	.15
930	.158
1920	.166
3660	.1765
4470	.203
5280	.2155
6060	.2265
6780	.239
7740	.257
8520	.280
9120	.3
9720	.312
10320	.325
10920	.343
11820	.3675
12300	.382
12720	.397
13140	.413
13560	.422
14070	.433
14460	.444
14880	.463
15300	.4775
15840	.4995
16280	.512
16680	.532
17100	.5455
17520	.566
17980	.577
18300	.5995
18720	.6215

593C
Specimen
Number
81-250

t	a
0	.168
1140	.175
2340	.185
4140	.217
5940	.25
6940	.268
7320	.281
7890	.287
8520	.308
8820	.314
9180	.326
9840	.3395
10440	.352
11040	.376
11640	.3925
12240	.410
12840	.425
13440	.4435
14040	.4735
14640	.4935
15240	.5185
15840	.54
16440	.572
17040	.6035

648C BASELINE DATA

81-231

0. .137
1592. .171
2177. .1863
2900. .2095
3080. .2275
3648. .259
3928. .2735
4135. .289
4290. .294
4472. .315
4600. .325
4789. .3335
4976. .344
5157. .371
5316. .388
5426. .3935
5556. .41
5648. .421
5901. .4365
5866. .4485
5956. .4585
6063. .475
6157. .484
6228. .5005
6288. .5035
6362. .5255
6418. .5265
6474. .5365
6532. .5515
6602. .5555
6652. .565
6706. .573
6776. .587
6841. .5915
6916. .606
6974. .613
7034. .62
7084. .6245
7148. .633
7214. .647
7276. .6585
7346. .674
7404. .688
7466. .695
7534. .708
7587. .722
7644. .732
7704. .754

81-242

0,0.142
60,0.141
1260,0.144
2460,0.146
3660,0.151
7260,0.169
9060,0.180
11010,0.190
12810,0.205
14610,0.222
16710,0.282
18810,0.353
20610,0.437
20730,0.453
22530,0.599
23120,0.651
23430,0.699
23730,0.739

TRANSITION DATA

Specimen Number 81-246 .

a = half total crack length (inches)

t = total time (seconds)

Start at 648C

Go to 537C

Go to 593C

t	a
240	.2945
330	.299
420	.3045
510	.319
600	.3425
690	.349
780	.357
870	.3685
960	.3905
1050	.4005
1140	.409
1230	.433
1320	.443
1410	.473

t	a
1500	.4755
1680	.4755
1920	.4775
2280	.4775
3000	.4785
3600	.4785
4900	.4835
6780	.493
8580	.495
11580	.4965
13380	.505
15960	.5085
17940	.5085
19860	.5135
22800	.514
26400	.532
28200	.5335
30000	.538
31380	.5455
34020	.5465
37320	.558
40560	.5595
42300	.5685
43920	.57
46440	.58
49200	.588
51780	.601
54720	.609
56700	.619
57900	.622
61500	.626
63300	.6275
64920	.6355

t	a
65010	.639
65100	.644
65190	.6485
65280	.6575
65400	.6605
65520	.669
65610	.6775
65700	.6825
65790	.688
65880	.7005
65970	.7015
66060	.714
66150	.723

TRANSITION DATA

Specimen Number 81-247

a = half total crack length (inches)
t = total time (seconds)

Start at 648C

Go to 593C

Go to 648C

t a

0,.163
90,.1685
180,.1715
270,.176
360,.179
450,.1855
540,.1905
660,.197
750,.2045
840,.208
930,.22
1020,.2275
1110,.235
1200,.2405
1280,.2515
1380,.2575
1470,.2705
1580,.277
1650,.2865
1740,.2975

t a

1850,.3005
1940,.3015
2030,.3045
2120,.307
2210,.3075
2300,.309
2390,.311
2510,.3125
2630,.3125
2750,.3135
2880,.3185
3170,.321
3680,.328
4190,.3325
4790,.3435
5390,.358
5870,.3615
6470,.368
7070,.38
7550,.3945
7970,.4055
8570,.4215
9170,.422
9770,.4355

t a

9860,.447
9950,.4645
10040,.475
10130,.495
10220,.5135
10310,.534
10400,.554
10490,.577
10580,.5885
10670,.6165
10760,.6415
10850,.6615
10940,.7005

TRANSITION DATA

Specimen Number 81-252

a = half total crack length (inches)
t = total time (seconds)

Start at 593C

Go to 648C

Go to 593C

t	a
0	.1915
900	.1955
1800	.206
2700	.2195
3600	.229
4500	.2485
5400	.287
6300	.284
6900	.2915

t	a
7200	.33
7800	.4335
8100	.4995
8220	.5255
8290	.549

t	a
8400	.561
8520	.5655
8640	.571
8760	.5795
8890	.5845
9000	.5885
9180	.5945
9350	.5995
9600	.6075
9840	.6165
10080	.620

TYPE 1 TESTS
48 SECOND CYCLE

Specimen Number	Specimen Number
81-217	81-244WA
t a	t a
0,.1575	0,.1525
240,.1575	1800,.1665
540,.1555	3240,.181
840,.1695	5040,.1905
1140,.171	6840,.1955
1620,.162	8640,.211
1920,.1625	10440,.222
2520,.175	11820,.2255
3120,.1765	13140,.236
3720,.190	17940,.2765
4920,.1915	19440,.2995
6120,.11945	20340,.302
7320,.219	21240,.3125
8520,.235	22140,.3295
9420,.235	
15720,.331	
16620,.3435	
17520,.366	
19120,.3715	
18720,.3895	
19320,.395	
19920,.412	
20520,.4145	
21120,.4295	
21720,.4465	
22320,.4565	
22920,.470	
23520,.4745	
24120,.482	
24720,.504	
25320,.516	
25920,.5295	
26520,.5605	
27120,.573	
27900,.5955	
28500,.602	
29100,.6185	
29790,.6395	
30600,.671	
31320,.7085	

TYPE 1 TESTS
132 SECOND CYCLE

a = half total crack length (inches)
t = total time (seconds)

Specimen
Number

81-240

Specimen
Number

81-227B

t a

0, .1445
720, .159
1440, .159
2220, .165
3120, .172
4020, .177
4920, .1915
5820, .2
7020, .214
8220, .231
8920, .238
9780, .25
10380, .2625
10980, .2725
11980, .294
12480, .307
13080, .3145
13680, .3265
14280, .3525
15480, .378
16080, .3955
16880, .411
17280, .4155
18480, .4635
19380, .5005
20280, .538
20880, .547
21540, .5695
22080, .6125
22980, .650
23580, .675

t a

0, .3725
660, .385
1260, .402
1560, .408
1860, .416
2460, .4375
2760, .449
3060, .4555
3360, .4635
3660, .478
4260, .498
4860, .523
5460, .5475
6060, .577
6660, .602
6960, .617
7260, .637
7560, .6505
7860, .662
8160, .683
8460, .7005
8760, .711
9060, .734

TYPE 1 TESTS
480 SECOND CYCLE

a = half total crack length (inches)
t = total time (seconds)

Specimen Number		Specimen Number
81-218		81-241WB
t	a	t a
0, .175		0, .4095
1200, .178		790, .4205
3300, .1945		1380, .4265
5400, .2205		1980, .4525
6780, .233		2580, .465
7980, .255		3180, .485
8700, .282		3780, .4955
9900, .299		4380, .521
10900, .2775		4980, .541
11700, .2845		5580, .566
12900, .311		6180, .577
13800, .3185		6780, .6
14700, .3285		7200, .6185
15800, .3485		7880, .6385
16800, .364		8100, .658
17700, .378		8580, .6735
18600, .397		9180, .7065
19700, .4195		9480, .72
20300, .428		
20900, .4535		
21500, .458		
22100, .472		
22700, .493		
23300, .507		
23900, .5195		
24500, .53		
25100, .5435		
25700, .5665		
26300, .585		
27020, .605		
27800, .623		
28480, .652		
29300, .6795		

TYPE 2 TEST

TYPE 3 TESTS

Specimen
Number
81-216
Hold for 3 min

t	a
0, .231	
1380, .31	
1680, .3235	
1980, .352	
2280, .3815	
2580, .4025	
2880, .44	
3180, .472	
3540, .512	
3780, .5385	
4080, .5825	
4380, .6255	
4580, .6585	
4740, .6815	
4920, .718	

Specimen
Number
81-214A
Hold for 3 min

t	a
0, .218	
1140, .218	
2340, .22	
5940, .2275	
8340, .24	
14040, .262	
17840, .2785	
20340, .284	
23040, .311	
25740, .318	
28440, .331	
30800, .345	
32400, .352	
34200, .368	
36000, .3755	
37800, .3785	
40200, .395	
45500, .4225	
48900, .427	
49000, .4385	
49200, .4495	
50480, .4535	
52380, .4675	
53460, .474	
55800, .495	
57000, .5105	
58500, .519	
59700, .5255	
60900, .535	
66540, .585	
67740, .597	
69940, .607	

Specimen
Number
81-246W
Hold for 15 min

t	a
0, .1595	
1900, .162	
3600, .1655	
7200, .172	
14400, .197	
8000, .2145	
21600, .229	
25200, .2495	
30800, .2825	
32480, .2995	
35280, .319	
37080, .3195	
39880, .3305	
44880, .376	
48480, .395	
50580, .4125	
52380, .4245	
54780, .444	
56580, .4635	
58380, .4775	
61380, .503	
64980, .54	

TYPE 4 TESTS

PROOF TEST

Specimen
Number

81-227A

Hold for 3 min

t a

0, .1985
300, .2045
600, .2075
1200, .217
1800, .2295
2400, .238
3000, .2515
3600, .263
4200, .279
4800, .296
5400, .311
5700, .3185
6000, .3325
6300, .341
6800, .3475
6900, .363
7200, .3805

Specimen
Number

81-217WA

Hold for 15 min

t a

0, .1775
2400, .1845
4200, .208
5400, .221
6300, .2375
7200, .256
8100, .264
9000, .2935
9900, .2995
10500, .332
11100, .3335
11700, .3415
12300, .3745
12900, .377

Specimen
Number

81-240W

t a

0, .1895
960, .1935
2450, .2015
3420, .218
8580, .2975
9900, .3215
10500, .337
11100, .352
11700, .372
12300, .383
12900, .3995
13550, .4125
14480, .446
15300, .4785
15900, .499
16500, .5195
16980, .5435
17400, .5525
17820, .5805
18300, .6085
18600, .621
18950, .672
19200, .6775
18900, .6995

Bibliography

1. Nicholas, T. and J. M. Larsen, "Life Prediction for Turbine Engine Components," Air Force Wright Aeronautical Laboratories, AFWAL/MLLN, Wright-Patterson AFB, OH.
2. Robinson, E. L., "Effect of Temperature Variation on the Long-Term Rupture Strength of Steels, ASME Transactions, 74: 777-781 (1952).
3. Miller, J., "Effect of Temperature Cycling on the Rupture Strength of High Temperature Alloys," Symposium on Effects of Cyclic Heating and Stressing on Metals at Elevated Temperatures, STP-165, American Society of Testing and Materials (ASTM), Philadelphia, 1954.
4. Carreker, R. P., J. G. Leschen, and J. D. Lubahn, "Transient Plastic Deformation," Transactions, American Institute of Mining and Metallurgical Engineers, 180: 139-146 (1949)
5. Rau, C. A., Jr., A. E. Gemma, and G. R. Leverant, "Thermal - Mechanical Fatigue Crack Propagation in Nickel - and Cobalt- Base Superalloys Under Various Strain - Temperature Cycles", Fatigue at Elevated Temperatures, ASTM STP-520, American Society for Testing and Materials, Philadelphia, 1973.
6. Shahinian, P. and K. Sadananda, "Crack Growth Behavior Under Creep-Fatigue Conditions in Alloy 718", Symposium on Creep-Fatigue Interaction, American Society of Mechanical Engineers, 1976.
7. Domas, P. A. and T. S. Cook, "Crack Propagation Under Thermal Mechanical Cycling", AFWAL-TR-81-4067. Wright-Patterson AFB, OH: Materials Laboratory (AFWAL/MLLN), Air Force Wright Aeronautical Laboratories, 1981.
8. Hartman, George A. III, University of Dayton Research Institute (developer of heating apparatus) Dayton, OH.
9. Beailieu, D., Structures Technology, Government Products Division, Pratt and Whitney Corporation (personal correspondence). West Palm Beach, Florida, July 19, 1983.
10. Donath, R. C., T. Nicholas, and L. S. Fu, "Experimental Investigation of Creep Crack Growth in IN-100", Fracture Mechanics: Thirteenth Conference, ASTM STP-743, American Society for Testing and Materials, Philadelphia, 1981.

Vita

Douglas Lee Miller was born on 19 March 1953 in Ellwood City, Pennsylvania. He graduated from high school in 1971 at Derry, Pennsylvania and attended the United States Air Force Academy. In 1975, he received the degree of Bachelor of Science, majoring in Engineering Mechanics, and also a commission in the USAF. He completed pilot training and received his wings in October 1976. He was transferred to Little Rock AFB, Arkansas where he served as a C-130 pilot and flight instructor in the 314th Tactical Airlift Wing. In June, 1982, Captain Miller entered the School of Engineering, Air Force Institute of Technology and he also completed a Master of Arts degree in Business Management from Websters College, Saint Louis, Missouri.

Permanent address: Route 19 Box 246

Hot Springs, Arkansas 71901

UNCLASSIFIED

SECURITY CLASSIFICATION OF THIS PAGE

REPORT DOCUMENTATION PAGE

1a. REPORT SECURITY CLASSIFICATION UNCLASSIFIED			1b. RESTRICTIVE MARKINGS	
2a. SECURITY CLASSIFICATION AUTHORITY			3. DISTRIBUTION/AVAILABILITY OF REPORT Approved for public release; distribution unlimited	
2b. DECLASSIFICATION/DOWNGRADING SCHEDULE				
4. PERFORMING ORGANIZATION REPORT NUMBER(S) AFIT/GAE/AA/83D-15			5. MONITORING ORGANIZATION REPORT NUMBER(S)	
6a. NAME OF PERFORMING ORGANIZATION School of Engineering		6b. OFFICE SYMBOL (If applicable) AFIT/ENY	7a. NAME OF MONITORING ORGANIZATION	
6c. ADDRESS (City, State and ZIP Code) Air Force Institute of Technology Wright-Patterson AFB, Ohio 45433			7b. ADDRESS (City, State and ZIP Code)	
8a. NAME OF FUNDING/SPONSORING ORGANIZATION		8b. OFFICE SYMBOL (If applicable)	9. PROCUREMENT INSTRUMENT IDENTIFICATION NUMBER	
8c. ADDRESS (City, State and ZIP Code)			10. SOURCE OF FUNDING NOS.	
			PROGRAM ELEMENT NO.	PROJECT NO.
			61102F	2307
			TASK NO.	WORK UNIT NO.
			P1	02
11. TITLE (Include Security Classification) See Box 19				
12. PERSONAL AUTHOR(S) Douglas L. Miller, B.S., M.A., Captain, USAF				
13a. TYPE OF REPORT MS Thesis	13b. TIME COVERED FROM _____ TO _____	14. DATE OF REPORT (Yr., Mo., Day) 1983 December	15. PAGE COUNT 80	
16. SUPPLEMENTARY NOTATION 3 JAN 1984 APPROVED FOR PUBLIC RELEASE LYNN E. WOLAVER Dean for Research and Professional Development Air Force Institute of Technology (AIG)				
17. COSATI CODES			18. SUBJECT TERMS (Continue on reverse if necessary and identify by block number)	
FIELD	GROUP	SUB. GR.		
20	11		Crack growth rate, Non-isothermal, Linear Cumulative Damage Modeling	
19. ABSTRACT (Continue on reverse if necessary and identify by block number) Title: SUSTAINED LOAD CRACK GROWTH IN INCONEL 718 UNDER NON-ISOTHERMAL CONDITIONS Thesis Chairman: George K. Haritos, Major, USAF				
20. DISTRIBUTION/AVAILABILITY OF ABSTRACT UNCLASSIFIED/UNLIMITED <input checked="" type="checkbox"/> SAME AS RPT. <input type="checkbox"/> DTIC USERS <input type="checkbox"/>			21. ABSTRACT SECURITY CLASSIFICATION UNCLASSIFIED	
22a. NAME OF RESPONSIBLE INDIVIDUAL George K. Haritos, Associate Professor			22b. TELEPHONE NUMBER (Include Area Code) (513) 255-2998	22c. OFFICE SYMBOL AFIT/ENY

DD FORM 1473, 83 APR

EDITION OF 1 JAN 73 IS OBSOLETE.

UNCLASSIFIED

SECURITY CLASSIFICATION OF THIS PAGE

This investigation found linear cumulative damage modeling applicable to creep crack growth under non-isothermal conditions. The best results are obtained for high crack growth rates produced either by high temperature (above 593C), or by high stress intensities (K greater than $50 \text{ MPa(m)}^{1/2}$). Except for one test, the linear model predicts conservative growth rates.

Constant temperature data are collected for 537, 593, and 648C and presented as da/dt vs K curves. Center-cracked specimens of Inconel 718 are used. The isothermal baseline data are used to predict crack growth rates for the non-isothermal tests using linear cumulative modeling. Specimens are subjected to low frequency thermal cycling between 537C and 648C. Constant load is always maintained throughout each test. Temperature is changed in the vicinity of the crack by using four infrared quartz halogen lamps. This allows realistic temperature changes in short periods of time, approximately 4.6C/second. A micro-computer maintains the desired temperature profile. Various hold times and temperature change rates are used.

The predicted creep crack growth rates were within a factor of two of the actual test data. The time-to-failure, predicted for one test, is 56 percent of the actual time to failure.

END

FILMED

2-84

DTIC